# Concatenated nicotinic acetylcholine receptors: A gift or a curse?

Philip Kiær Ahring,* Vivian Wan Yu Liao,* and Thomas Balle

Faculty of Pharmacy, The University of Sydney, Sydney, Australia

Nicotinic acetylcholine receptors (nAChRs) belong to the Cys-loop receptor family and are vital for normal mammalian brain function. Cys-loop receptors are pentameric ligand-gated ion channels formed from five identical or homologous subunits oriented around a central ion-conducting pore, which result in homomeric or heteromeric receptors, respectively. Within a given Cys-loop receptor family, many different heteromeric receptors can assemble from a common set of subunits, and understanding the properties of these heteromeric receptors is crucial for the continuing quest to generate novel treatments for human diseases. Yet this complexity also presents a hindrance for studying Cys-loop receptors in heterologous expression systems, where full control of the receptor stoichiometry and assembly is required. Therefore, subunit concatenation technology is commonly used to control receptor assembly. In theory, this methodology should facilitate full control of the stoichiometry. In reality, however, we find that commonly used constructs do not yield the expected receptor stoichiometries. With ternary or more complex receptors, concatenated subunits must assemble uniformly in only one orientation; otherwise, the resulting receptor pool will consist of receptors with mixed stoichiometries. We find that typically used constructs of α4β2 nAChR dimers, tetramers, and pentamers assemble readily in both the clockwise and the counterclockwise orientations. Consequently, we investigate the possibility of successfully directing the receptor assembly process using concatenation. We begin by investigating the three-dimensional structures of the α4β2 nAChR. Based on this, we hypothesize that the minimum linker length required to bridge the C terminus of one subunit to the N terminus of the next is shortest in the counterclockwise orientation. We then successfully express receptors with a uniform stoichiometry by systematically shortening linker lengths, proving the hypothesis correct. Our results will significantly aid future studies of heteromeric Cys-loop receptors and enable clarification of the current contradictions in the literature.

## INTRODUCTION

There could be several reasons for using concatenated subunits to expres heteromeric Cys-loop receptors. However, this technique is mostly used to direct receptor assembly to ensure expression of specific receptor pools. For instance, binary receptor combinations such as the nicotinic acetylcholine (ACh) receptor (nAChR) α4β2 can express as either $(\alpha4)_3(\beta2)_2$ or $(\alpha4)_2(\beta2)_3$. By using concatenated subunits, the cell surface receptor pool can be enriched with either combination (Zhou et al., 2003; Harpsøe et al., 2011). Because concatenated constructs could consist of anywhere between two to five subunits (dimers to pentamers), this technique promises unique control of the assembly process at the single-receptor level.

As Cys-loop subunits have their C and N termini in the extracellular space, it is a straightforward process to concatenate them. This consists of manipulating the respective cDNAs such that all coding regions are located in the same expression cassette as one open reading frame. This is attained using a synthetic linker sequence bridging the C terminus of the first subunit to the N terminus of the next subunit. Typical linker sequences code for glutamine repeats or alanine–glycine–serine (AGS) repeats, as these amino acids are believed to have relatively minimal impact on normal subunit folding. Baumann et al. (2001) demonstrated that functional α1β2γ2 γ-amino-butyric-acid type A receptors ($GABA_ARs$) formed readily in *Xenopus laevis* oocytes upon the injection of concatenated dimer constructs of α1 and β2 in combination with a monomeric γ2 subunit. Later, Zhou et al. (2003) demonstrated successful expression of α4β2 nAChRs using a similar methodology. The most simple and efficient construct strategy used six repeats of an AGS sequence to link the β2 to the α4 subunit ($\beta2\text{-}(AGS)_6\text{-}\alpha4$). This was paired with the expression of either a monomeric α4 or β2 subunit. The specific methodologies developed in these studies have since been used extensively to answer basic scientific questions for both $GABA_ARs$ and nAChRs (Baumann et al., 2002; Kuryatov and Lindstrom, 2011; Mazzaferro et al., 2011; Shu et al., 2012). For ease, the $\beta2\text{-}(AGS)_6\text{-}\alpha4$ construct is termed the β-6-α construct in this paper.

Although the use of concatenated constructs is a powerful technique to study Cys-loop receptors, there are potential caveats that could affect experimental outcomes. First, the artificial linker sequence and accompanying structural constraints could change the

*P.K. Ahring and V.W.Y. Liao contributed equally to this paper.
Correspondence to Philip Kiær Ahring: philip.ahring@sydney.edu.au



The Rockefeller University Press
J. Gen. Physiol. 2018 Vol. 150 No. 3 453–473
https://doi.org/10.1085/jgp.201711846

receptor properties. Although this has not been commonly observed, results should be verified using other methodologies whenever possible. Second, the linker sequences could be subjected to proteolysis, thereby freeing subunits to assemble in an unintended manner. Although proteolysis never can be fully excluded, this has fortunately not been found to occur to any significant extent (Groot-Kormelink et al., 2006; Carbone et al., 2009). Third, linked constructs could form unexpected and unwanted receptors by themselves, thereby "polluting" the receptor pool. Indeed, such unwanted receptors are regularly observed; hence, linked dimer, trimer, or tetramer constructs should ideally be constructed such that they do not form functional receptors by themselves (Zhou et al., 2003; Groot-Kormelink et al., 2004; Kaur et al., 2009). Fourth, the assembly direction may not be fully controlled. This means several different receptor stoichiometries can arise in ternary receptor scenarios. Of the caveats listed above, we find the fourth to be the most disconcerting, as it can potentially lead to erroneous conclusions.

Therefore, in the present study, we explore the degree to which the commonly used nAChR β2-6-α4 construct directs receptor subunit orientation. Unexpectedly, β2-6-α4 did not direct the orientation of linked subunits, nor did derived tetrameric or pentameric constructs. Because the β2-6-α4 construct is the "mother" of most used nAChR constructs, the implications of this are substantial. Furthermore, our data trigger the question of whether it is at all possible to direct subunit orientation using linked subunits. To address this, we studied 3-D models of Cys-loop receptor subunits and hypothesized that short linkers would direct receptor assembly in the counterclockwise orientation. We then designed a range of concatenated constructs with shorter linkers. Importantly, we found that although it is possible to direct subunit orientation, this first requires an optimization process to identify the "optimal" linker length for the specific subunits in question. This optimization, however, is a crucial step for the appropriate use of concatenation technology.

## MATERIALS AND METHODS

### Materials

3-(3-(pyridine-3-yl)-1,2,4-oxadiazol-5-yl)benzonitrile (NS9283) was synthesized at Saniona A/S as described by Timmermann et al. (2012). The structure was confirmed using mass spectrometric analysis and proton nuclear magnetic resonance spectroscopy and was of >98% purity. ACh and all salts or other chemicals not specifically mentioned were purchased from Sigma-Aldrich and were of analytical grade. Oligonucleotides were purchased from Sigma-Aldrich, and sequencing services were obtained from the Australian Genome Research Facility. Restriction enzymes, Q5 polymerase, T4 DNA ligase, and competent *Escherichia coli* 10-β bacteria were from New England Biolabs.

### Molecular biology

Human cDNA for monomeric α4, β2, and $\alpha4^{VFL}$ nAChR subunits and concatenated constructs β2-6-α4 and β2-6-α4-9-β2-6-α4 were kind gifts from Saniona A/S. New β2-xa-α4 concatenated constructs, where x = 9, 6, 3, 0, and −3 amino acid (a) linkers, were built from wild-type β2 and α4 subunits using PCR. In brief, AGS linker sequences were designed to contain a unique central restriction site; antisense β2 and sense α4 oligonucleotide sequences were then fabricated to traverse this site. The antisense β2 oligonucleotides caused deletion of the β2 stop codon and in-frame fusion to the AGS linker sequence. The sense α4 oligonucleotides caused omission of the α4 signal peptide and in-frame fusion to the AGS linker sequence. The remaining β2 sense and α4 antisense oligonucleotides were designed to match the respective wild-type sequences and include suitable restriction sites. Standard PCR reactions with β2 or α4 as a template were performed using Q5 polymerase, and PCR products were cloned into in-house vectors using restriction digestion and ligation. Correct introduction of linker sequences and fidelity of all coding sequences were verified by double-stranded sequencing. Thereafter, concatenated constructs were created by restriction digestion and ligation using the unique AGS linker and vector sites. Pentameric constructs were built in a similar manner, with each linker sequence containing its own unique restriction site. *E. coli* 10-β bacteria were used as hosts for plasmid expansion, and plasmid purifications were performed with standard kits (Qiagen). cRNA was produced from linearized cDNA using the mMESSAGE mMACHINE T7 Transcription kit (Ambion) according to the manufacturer's description and stored at −80°C until use.

### Modeling

The x-ray structure of the human α4β2 nAChR (Protein Data Bank accession no. 5KXI; Morales-Perez et al., 2016) was downloaded from the database (Berman et al., 2002) and prepared according to the protocol for protein preparation implemented in Maestro 10.4 (Schrödinger Release 2015–4; Schrödinger). In the published structure, 20 amino acids in the C-terminal end of the β2 subunit are disordered and are hence unresolved. Thus, relative to the wild-type protein, the β2 subunit chain ends with $FLQPL^{373}$, and $^{374}FQNYTTTTF$ $LHSDHSAPSSK^{393}$ is missing. No attempts were made to model these missing residues. Instead, the shortest possible AGS-repeat linkers were inserted to create a clockwise construct linking the last visible residue in the C-terminal tail of the β2 subunit (chain B) to the N-terminal tail of the α4 subunit (chain A) or a counterclockwise construct connecting the last visible C-ter-

minal residue of β2 (chain E) to the N terminus of α4 (chain A). In both cases, "shortest possible" was defined as the number of AGS repeats required to link the two terminals without causing significant distortion to either terminal after geometry optimization in a Macromodel (OPLS3 Force Field, GB/SA solvation model).

### Electrophysiology

*X. laevis* oocytes were prepared as previously described by Mirza et al. (2008). In brief, to obtain isolated oocytes, lobes from the ovaries of adult female *X. laevis* frogs were removed as approved by the Animal Ethics Committee of The University of Sydney (reference number 2013/5915) and defolliculated using collagenase. Oocytes were injected with ∼50 nl of a 0.5-µg/µl cRNA mixture encoding the desired nAChR subunits and incubated for 2–3 d (unless otherwise noted) at 18°C in modified Barth's solution (96 mM NaCl, 2.0 mM KCl, 1 mM $MgCl_2$, 1.8 mM $CaCl_2$, 5 mM HEPES, 2.5 mM sodium pyruvate, 0.5 mM theophylline, and 100 µg/ml gentamycin, pH 7.4). Electrophysiological recordings using the two-electrode voltage-clamp technique were performed with oocytes placed in a custom-built recording chamber and continuously perfused with a $Ca^{2+}$-free saline solution termed CF buffer (115 mM NaCl, 2.5 mM KCl, 1.8 mM $BaCl_2$, and 10 mM HEPES, pH 7.4). Pipettes were backfilled with 3 M KCl, and open pipette resistances ranged from 0.4 to 2 MΩ when submerged in CF buffer. Cells were voltage clamped at a holding potential of −60 mV using an Axon Geneclamp 500B amplifier (Molecular Devices). Oocytes with initial leak currents exceeding 200 nA when clamped were discarded. NS9283 was dissolved as a 100-mM stock solution in DMSO, which upon final dilution gave a maximal concentration of 0.1%. This DMSO concentration did not evoke any measurable currents from wild-type α4β2 receptors. Fresh ACh and NS9283 dilutions were prepared in CF buffer on the day of the experiment, and solutions were applied to the oocytes with a flow rate of 2.0 ml/min via a glass capillary. Each application lasted ∼30 s, and the application system ensured rapid solution exchange (in the order of a few seconds). Amplified signals were low-pass filtered at 20 Hz, digitized at 200 Hz by an Axon Digidata 1440A (Molecular Devices), and recorded using Clampex 10.2 (Molecular Devices).

### Experimental protocols

A complete concentration–response relationship (CRR) consisting of six to eight individual concentrations of NS9283 or ACh was obtained from each oocyte. To ensure the reproducibility of evoked current amplitudes, a set of control applications was performed before the actual concentration–response applications. These control applications were three $ACh_{control}$ (10 µM) applications, one $ACh_{max}$ (3,160 µM) application, another three $ACh_{control}$ (10 µM) applications, and finally a buffer (no ACh) application. Thereafter followed six to eight applications of NS9283 coapplied with $ACh_{control}$ (10 µM) or ACh alone in increasing concentrations. In a few instances, an NS9283 CRR was obtained after an ACh CRR on the same oocyte. In these cases, the maximal ACh-evoked current amplitude for the given oocyte was considered as belonging only to the ACh CRR. Final datasets for NS9283 and ACh were assembled from experiments conducted on a minimum of two batches of oocytes.

### Data analysis

Raw traces were analyzed using pClamp 10.2 (Molecular Devices). Traces were baseline subtracted during analysis, and responses to individual applications were quantified as peak current amplitudes. For experiments with ACh, peak current amplitudes (I) of full CRRs were fitted to the Hill equation and normalized to the maximal fitted response ($I_{max\_fit\_ACh}$) for each individual oocyte (i.e., $I/I_{max\_fit\_ACh}$). For experiments with NS9283, the compound was coapplied with $ACh_{control}$ (10 µM). Differences between $ACh_{control}$-evoked current amplitudes in the absence or presence of NS9283 (I) were calculated as the percent change from the $ACh_{control}$-evoked current (i.e., $([I-I_{ACh\_control}] \times 100)/I_{ACh\_control}$). All CRRs were fitted by nonlinear regression in Prism 7 (GraphPad) to a mono- or biphasic equation with a constrained Hill slope of 1 and efficacy at infinitely low compound concentrations set to 0, unless otherwise specified. Comparison of best approximation (monophasic vs. biphasic) was performed using the F test in Prism 7. Further statistical analysis was performed using Prism 7.

### Experimental strategy 1: ACh and NS9283 sensitivity of α4β2 nAChRs

Depending on the stoichiometry, wild-type α4β2 nAChRs display either a monophasic $(\alpha4)_2(\beta2)_3$ or a biphasic $(\alpha4)_3(\beta2)_2$ ACh CRR, meaning that the data are best approximated by a first- or second-order equation as revealed by, for example, an F test (Fig. 1, A and B; Harpsøe et al., 2011; Mazzaferro et al., 2011). For the biphasic $(\alpha4)_3(\beta2)_2$ receptor concentration–response curve, the first component reflects ACh binding and activation via two high-affinity α4–β2 interface–binding sites, and the second component reflects the additional activation of the same receptors via ACh binding to the low-affinity α4–α4 interface site (Indurthi et al., 2016). Such biphasic CRRs with interdependent variables are, however, inherently difficult to resolve, and the calculated fractions of the first component, as well as $EC_{50}$ values, can vary considerably from relatively minor data variations. Hence, it can be virtually impossible to distinguish a pure receptor pool from one containing pollutant receptors whenever biphasic CRRs are involved.

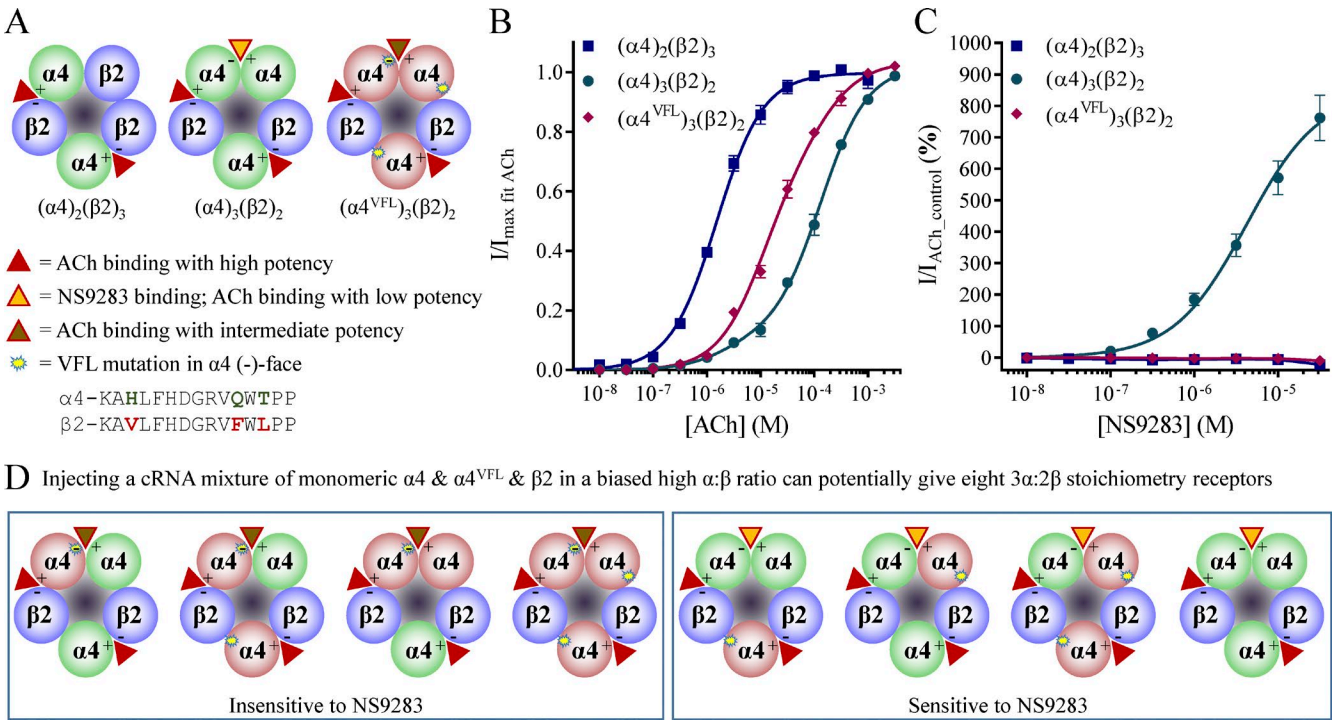


Figure 1. **α4β2 nAChR stoichiometry and functional effects of ACh and NS9283.** *X. laevis* oocytes were injected with cRNA mixtures of α4 and β2 or $α4^{VFL}$ and β2 subunits in 10:1 ratios and subjected to two-electrode voltage-clamp electrophysiology as described in Materials and methods. The 10:1 cRNA ratios were used to ensure uniform populations of $(α4)_3(β2)_2$ and $(α4^{VFL})_3(β2)_2$ receptors. Data for α4 and β2 injected in a 1:4 ratio ($(α4)_2(β2)_3$ receptor) are from Harpsøe et al. (2011). **(A)** Functional α4β2 nAChRs can express in 2α:3β or 3α:2β stoichiometries (left and middle, respectively). The stoichiometry affects the total number of ACh-binding sites, as the 3α:2β stoichiometry contains an additional site in the α4–α4 interface. Furthermore, NS9283 binds with high selectivity in the α4–α4 site, where it behaves as an agonist. Upon mutating three amino acids in the complementary face of the α4 subunit to give $α4^{VFL}$, ACh sensitivity is increased in the $α4^{VFL}$–$α4^{VFL}$ site, and NS9283 binding is lost (right). **(B)** ACh CRRs. Baseline-subtracted, ACh-evoked peak current amplitudes (I) for the indicated receptors were fitted to the Hill equation by nonlinear regression and normalized to the maximal fitted values ($I_{max\ fit\ ACh}$). Normalized responses are depicted as means ± SEM as a function of the ACh concentrations, and they are fitted to biphasic equations with a fixed bottom of 0 and a Hill slope of 1. Data were obtained from *n* = 9–14 experiments, and regression results are presented in Table 1. Data for the $(α4)_2(β2)_3$ receptor are from Harpsøe et al. (2011). **(C)** NS9283 CRRs. NS9283 enhancement of ACh-evoked currents was evaluated for $(α4)_3(β2)_2$ and $(α4^{VFL})_3(β2)_2$ receptors by coapplication with a submaximal control concentration of ACh (10 µM). Baseline-subtracted peak current amplitudes (I) were expressed as percent change from $I_{ACh\_control}$ and are depicted as means ± SEM as a function of the NS9283 concentration. Data points were fitted by nonlinear regression to the Hill equation with a fixed bottom of 0 and a Hill slope of 1. Data were obtained from *n* = 13–16 experiments, and regression results are presented in Table 1. Data for the $(α4)_2(β2)_3$ receptor are from Timmermann et al. (2012). **(D)** Hypothetically, injection of a cRNA mixture of α4, $α4^{VFL}$, and β2 into oocytes could yield eight different receptors in the 3α:2β stoichiometry. Using NS9283 as a marker, these can be divided into those that are sensitive and those that are insensitive, depending on whether the $α4^{VFL}$ subunit is participating in the complementary position of the α4–α4 interface.

To increase the assay sensitivity in the present work, we used the unique actions and binding property of the compound NS9283. Although originally identified as an allosteric modulator of α4β2 receptors, NS9283 has been found to have site-selective agonistic actions (Timmermann et al., 2012; Olsen et al., 2013, 2014). Essentially, NS9283 binds in the wild-type α4–α4 ACh-binding pocket, where it largely interacts with the same amino acids as ACh (Fig. 1 A). Thus, at nonsaturating ACh concentrations, NS9283 binding to the α4–α4 interface causes increased receptor activation of $(α4)_3(β2)_2$ receptors (Fig. 1 C and Table 1). However, NS9283 displays no actions on receptors that lack an α4–α4 interface, and because $(α4)_2(β2)_3$ receptors have a β2–β2 interface instead, no activity is observed at this stoichiometry.

### Experimental strategy 2: Using the combination of NS9283 and $α4^{VFL}$

Potent binding and efficacy of NS9283 are dependent on the presence of three E-loop amino acids (H142, Q150, and T152) in the complementary face of the α4 subunit (Olsen et al., 2014). Therefore, by point mutating these to the corresponding amino acids in β2 (V136, F144, and L146 [the VFL motif]), no NS9283 efficacy is observed in receptors with an $α4^{VFL}$–$α4^{VFL}$ interface (Fig. 1, A and C). Yet, these same three mutations cause the agonist-binding pocket in the $α4^{VFL}$–$α4^{VFL}$ interface

Table 1. **Maximal fitted response and potency of ACh and NS9283 from wild-type and concatenated α4β2 nAChRs**

| Construct | Subunit | ACh | | | | | NS9283 | | | | Both |
|---|---|---|---|---|---|---|---|---|---|---|---|
| | | $E_{max}$ | $pEC_{50\_1}$ | $pEC_{50\_2}$ | Frac | *n* | $E_{31.6\ \mu M}$ | $E_{max}$ | $pEC_{50}$ | *n* | $ACh_{max}$ current |
| | | % | | | | | % | % | | | *nA* |
| α4 (10:1) | β2 | 102 ± 1 | 5.7 ± 0.3 | 3.9 ± 0.04 | 0.11 ± 0.03 | 14 | 760 ± 70 | 860 ± 60 | 5.3 ± 0.1 | 13 | 8,100 ± 900 (27) |
| $α4^{VFL}$ (10:1) | β2 | 104 ± 2 | 5.0 ± 0.1 | 3.9 ± 0.3 | 0.71 ± 0.12 | 9 | −9.9 ± 1.8 | No pos. pot. | N/A | 16 | 1,700 ± 300 (25) |
| β-6-α | | 102 ± 2 | 5.8 ± 0.3 | 3.6 ± 0.1 | 0.11 ± 0.02 | 9 | 640 ± 90 | 900 ± 140 | 4.9 ± 0.2 | 9 | 1,000 ± 300 (18) |
| β-6-α | α4 | 101 ± 2 | 5.7 ± 0.6 | 3.8 ± 0.1 | 0.073 ± 0.038 | 10 | 860 ± 100 | 1,100 ± 100 | 5.1 ± 0.2 | 12 | 5,200 ± 800 (22) |
| β-6-α | $α4^{VFL}$ | 106 ± 2 | 5.2 ± 0.2 | 3.8 ± 0.1 | 0.40 ± 0.08 | 12 | 210 ± 20 | 270 ± 30 | 5.0 ± 0.1 | 7 | 2,200 ± 400 (19) |
| β-6-α (1:25) | $α4^{VFL}$ | 106 ± 1 | 5.3 ± 0.1 | 4.0 ± 0.1 | 0.39 ± 0.05 | 8 | 240 ± 20 | 300 ± 30 | 5.1 ± 0.1 | 6 | 1,200 ± 200 (12) |
| β-9a-α | | 105 ± 3 | 5.7 ± 0.2 | 3.9 ± 0.1 | 0.28 ± 0.05 | 11 | 100 ± 20 | 130 ± 30 | 5.0 ± 0.3 | 5 | 220 ± 60 (16) |
| β-9a-α | α4 | 103 ± 3 | 5.6 ± 0.4 | 3.7 ± 0.1 | 0.13 ± 0.05 | 8 | 680 ± 40 | 950 ± 80 | 4.9 ± 0.1 | 6 | 3,000 ± 600 (14) |
| β-9a-α | $α4^{VFL}$ | 109 ± 5 | 5.3 ± 0.3 | 3.7 ± 0.2 | 0.32 ± 0.09 | 5 | 200 ± 10 | 260 ± 20 | 5.0 ± 0.1 | 8 | 2,600 ± 1,000 (13) |
| β-6a-α | | 103 ± 2 | 5.8 ± 0.1 | 4.5 ± 0.4 | 0.70 ± 0.12 | 6 | 45 ± 9 | 51 ± 7 | 5.4 ± 0.2 | 6 | 94 ± 18 (12)[a] |
| β-6a-α | α4 | 100 ± 1 | 6.1 ± 0.4 | 3.9 ± 0.04 | 0.059 ± 0.018 | 10 | 710 ± 50 | 870 ± 60 | 5.1 ± 0.1 | 6 | 1,800 ± 300 (16) |
| β-6a-α | $α4^{VFL}$ | 105 ± 3 | 5.6 ± 0.4 | 4.2 ± 0.2 | 0.31 ± 0.14 | 7 | 140 ± 10 | 180 ± 10 | 5.0 ± 0.1 | 8 | 170 ± 40 (15) |
| β-3a-α | | 103 ± 1 | 5.7 ± 0.1 | 4.5 ± 0.2 | 0.64 ± 0.11 | 14 | 7.5 ± 8.2 | Inconclusive | N/A | 11 | 120 ± 30 (25)[b] |
| β-3a-α | α4 | 102 ± 1 | 5.7 ± 0.2 | 4.0 ± 0.03 | 0.11 ± 0.02 | 17 | 610 ± 30 | 720 ± 30 | 5.2 ± 0.1 | 18 | 1,500 ± 200 (35) |
| β-3a-α | $α4^{VFL}$ | 104 ± 1 | 5.7 ± 0.1 | 4.4 ± 0.1 | 0.41 ± 0.06 | 17 | 22 ± 3 | 27 ± 4 | 5.2 ± 0.2 | 24 | 890 ± 130 (41) |
| β-0a-α | | N/A | N/A | N/A | N/A | N/A | N/A | N/A | N/A | N/A | 15 ± 4 (24)[c] |
| β-0a-α | α4 | 103 ± 2 | 5.8 ± 0.7 | 3.7 ± 0.05 | 0.053 ± 0.028 | 11 | 840 ± 90 | 1,100 ± 100 | 5.0 ± 0.1 | 9 | 130 ± 40 (20)[d] |
| β-0a-α | $α4^{VFL}$ | 101 ± 1 | 5.4 ± 0.5 | 4.6 ± 0.2 | 0.28 ± 0.34 | 14 | −6.0 ± 2.4 | No pos. pot. | N/A | 15 | 95 ± 18 (29)[d] |
| β-(-3a)-α | | N/A | N/A | N/A | N/A | N/A | N/A | N/A | N/A | N/A | No current (18) |
| β-(-3a)-α | α4 | N/A | N/A | N/A | N/A | N/A | N/A | N/A | N/A | N/A | 36 ± 6 (27) |
| β-(-3a)-α | $α4^{VFL}$ | N/A | N/A | N/A | N/A | N/A | N/A | N/A | N/A | N/A | 15 ± 2 (21) |

*X. laevis* oocytes were injected with the indicated cRNA mixtures in a 1:1 ratio (unless otherwise indicated) and subjected to two-electrode voltage-clamp electrophysiology after 2–3 d of incubation time as described in Materials and methods; also see Fig. 1. Data points were fitted to either a monophasic or a biphasic equation with the bottom set to 0 and a Hill slope set to 1 by nonlinear regression. For ACh, biphasic fitting represented the preferred model for all datasets as determined by an F test. Fitted maximal responses of ACh and NS9283 are presented as $E_{max}$ ± SEM in percentages, with associated potencies presented as $pEC_{50}$ ± SEM in M for the indicated number of individual oocytes. Observed NS9283 responses at the 31.6-μM concentration are presented as $E_{31.6\ \mu M}$ ± SEM in percentages. The mean maximal current obtained with applications of 3.16 mM ACh is presented as $ACh_{max}$ current ± SEM in nanoamperes for all tested oocytes for each construct. N/A, not applicable; No pos. pot., no positive potentiation; Inconclusive, meaningful fitting not possible, as only ∼50% of the oocytes displayed a positive NS9283 response.

[a]Selected oocytes due to low $ACh_{max}$-evoked current amplitudes.

[b]No $ACh_{max}$-evoked currents in approximately three out of four oocytes.

[c]Only two oocytes show >25 nA $ACh_{max}$-evoked current amplitude.

[d]Mixture of oocytes from 3 and 5 d of incubation.

to resemble that of an α4–β2 interface, which leads to increased sensitivity of the second component of the ACh concentration–response curve (Fig. 1 B). Although NS9283 shows no activity at $(α4^{VFL})_3(β2)_2$ receptors, the situation is more complex when only one of the subunits is mutated in the α4–α4 interface. In the case of an $α4^{VFL}$–α4 interface, the VFL mutations do not face the NS9283-binding site, and therefore the compound still shows full response (Fig. 1 D). Conversely, in the case of an α4–$α4^{VFL}$ interface, the three VFL mutations face the NS9283-binding pocket, and NS9283 no longer binds with sufficient potency to allow any activity (Fig. 1 D). Therefore, NS9283 can be used to pinpoint the position of the $α4^{VFL}$ subunit in an α4–α4 interface; if NS9283 displays efficacy, the mutant $a4^{VFL}$ subunit is primary; if not, the subunit is complementary.

### Experimental strategy 3: Concentrations at which NS9283 shows selectivity

Like most other compounds, NS9283 only remains selective in a certain concentration range. At concentrations <10 μM, NS9283 appears fully selective for the α4–α4 interface. This is evidenced by the increasing current amplitudes at the $(α4)_3(β2)_2$ receptor in the presence of $ACh_{control}$ (10 μM) and the lack of actions at $(α4)_2(β2)_3$ or $(α4^{VFL})_3(β2)_2$ receptors (Fig. 1 C). At concentrations of 31.6 μM or higher, NS9283 still shows increased activity at $(α4)_3(β2)_2$ receptors; however, this is accompanied by inhibition of the $ACh_{control}$-evoked current amplitudes at $(α4)_2(β2)_3$ and $(α4^{VFL})_3(β2)_2$ receptors (Fig. 1 C). For $(α4^{VFL})_3(β2)_2$ receptors, an inhibition of −9.9 ± 1.8% ($n$ = 16) and −27 ± 2% ($n$ = 9) is observed at 31.6 and 100 μM, respectively (note, the 100-μM data point is not included in the illustration). Given that NS9283 binds to *Ls*-AChBP with a $K_i$ value of 67 μM (Olsen et al., 2014), the observed inhibition is consistent with binding to the ACh-binding pocket in α4–β2 interfaces at high concentrations. As NS9283 is not an agonist at the wild-type α4–β2 interfaces (Olsen et al., 2014), such binding would lead to competitive antagonism instead. Therefore, in the experiments performed in this study, we used a maximal concentration of 31.6 μM NS9283. This represents a compromise between the desire to observe

the highest possible activity in receptor pools with a high proportion of sensitive receptors and the desire to avoid inhibition in pools with a low proportion of sensitive receptors.

### Experimental strategy 4: Evaluating NS9283 efficacy at a fixed $ACh_{control}$ concentration

When comparing efficacy of a modulatory compound at different receptor types in the presence of an agonist, it is best practice to measure at the same open-channel probability (Ahring et al., 2016). In cases where the maximal open-channel probability is not known, it is usually approximated by using the same degree of agonist response (e.g., $EC_{10}$). However, this strategy is only valid when comparing efficacies between receptor populations that can be assumed uniform.

In this study, the response of NS9283 was measured at receptors arising from a range of constructs. One of the key findings was that many of these constructs did not lead to uniform receptor expression but to mixed receptor pools. These receptor pools contained both NS9283-sensitive and NS9283-insensitive receptors. To further complicate the situation, the receptors had variant ACh sensitivity. In such scenarios, a difference in measured NS9283 response is (a) a reflection of the change in the mean ACh CRR such that a given ACh concentration leads to altered percent activation (e.g., $EC_{10}$ to $EC_{30}$) and (b) a reflection of a change in percentage of NS9283-sensitive receptors among nonsensitive ones. Therefore, an attempt to adjust the $ACh_{control}$ concentrations according to ACh CRRs in cases with mixed receptor pools is counterproductive. Finally, it is important to note that a main goal in this study was to develop a technology that allows expression of pure receptor populations. Consequently, the specific experiments were designed such that this is achieved when NS9283 displays no efficacy.

## RESULTS

In the present study, we relied on the unique selectivity of NS9283 in combination with an NS9283-resistant mutant $\alpha4^{VFL}$ subunit to decipher the absolute stoichiometry of expressed α4β2 nAChRs. NS9283 selectively binds in the α4–α4 interface of wild-type $(\alpha4)_3(\beta2)_2$ receptors to increase receptor gating at submaximal ACh concentrations. The three mutations in the $\alpha4^{VFL}$ subunit make the ACh-binding pocket in an $\alpha4^{VFL}$–$\alpha4^{VFL}$ interface resemble that of an α4–β2 interface, increasing ACh sensitivity but abolishing NS9283 sensitivity (Fig. 1 A). Further detail regarding the selectivity of NS9283, its sensitivity to the VFL mutations, and the reason why NS9283 responses are compared for the 31.6-µM concentration in these results is presented in Materials and methods (Experimental strategies 1–4).

### Binary and ternary receptors

Heterologously expressed Cys-loop receptors often assemble in multiple stoichiometries. It is therefore imperative to consider what to expect in a situation when a receptor pool contains two or more receptor subpopulations. Expressing binary α4β2 nAChRs in oocytes by injection of wild-type α4 and β2 cRNA is simple because there are only two stoichiometries, 2α:3β and 3α:2β, that form functional receptors (Fig. 1 A; Harpsøe et al., 2011; Mazzaferro et al., 2011). Although injection of equimolar amounts of cRNA generally leads to a mixed receptor pool, biasing cRNA ratios allows for uniform receptor pool formation (Zwart and Vijverberg, 1998; Harpsøe et al., 2011). Using this methodology, α4β2 receptors were expressed in 2α:3β and 3α:2β stoichiometries by coinjection of α4 and β2 cRNA in 1:4 and 10:1 ratios, respectively. These two receptor pools are easily distinguished by their sensitivity to ACh and NS9283 (Fig. 1, B and C; and Table 1). Although the ACh CRR for the 2α:3β stoichiometry was well approximated by the Hill equation (i.e., a monophasic, or first-order, equation), the ACh CRR for the 3α:2β stoichiometry was best approximated by a biphasic, or second-order, equation. Furthermore, although 31.6 µM NS9283 displayed no positive response at the 2α:3β stoichiometry, the response at the 3α:2β stoichiometry was 760%. The binary scenario with a mutant $\alpha4^{VFL}$ subunit coinjected with wild-type β2 cRNA in a 10:1 ratio displayed ACh sensitivity intermediate to that of the two wild-type stoichiometries, although no positive efficacy was observed with NS9283 (Fig. 1, B and C; and Table 1). These data are in good agreement with previous studies (Harpsøe et al., 2011; Timmermann et al., 2012; Olsen et al., 2013).

Expression of ternary scenarios is inherently more complex. Even when biasing toward the 3α:2β stoichiometry, injection of a cRNA mixture consisting of wild-type α4, mutant $\alpha4^{VFL}$, and wild-type β2 can theoretically lead to assembly of eight different receptors that contain zero to three $\alpha4^{VFL}$ subunits (Fig. 1 D). It is rarely possible to distinguish these receptors from one another. By using NS9283 sensitivity as an assessment, they can be separated into two groups depending on the characteristics of the α4–α4 interface, as described in Materials and methods (Experimental strategy 2). Consequently, for ternary receptor scenarios, a concatenation methodology represents the only avenue to ensure receptor expression of specific stoichiometries.

### The linker in the β2-6-α4 concatenated construct does not direct the orientation of linked subunits

In our initial studies with linked subunits, we employed the widely used concatenated β2-6-α4 dimer construct (Zhou et al., 2003). As previously described, this particular construct contains a linker of six AGS repeats connecting the C terminus of the β2 to the mature N terminus of the α4 subunit.

β-6-α. Robust ACh-evoked currents with amplitudes in the microampere range were observed from oocytes injected with β-6-α cRNA alone (Table 1). For ACh, the CRR was best approximated with a biphasic equation, revealing two $EC_{50}$ values of ∼2 and 250 µM and a first component fraction of 0.11 (Fig. 2 A and Table 1). Furthermore, 31.6 µM NS9283 increased the $ACh_{control}$ (10 µM) current by 640% (Fig. 2, B and C; and Table 1). These data are similar to observations at the wild-type 3α:2β receptors obtained from α4 and β2 in the biased 10:1 cRNA ratio described in the previous section (*t* test NS9283 response: P = 0.30). This indicates that injection of the dimer construct alone leads to receptors that are predominantly of the 3α:2β stoichiometry, which is corroborated by the findings of Jin and Steinbach (2011) using a similar β-6-α construct. Disregarding the possibility of linker proteolysis, the simplest explanation for the observations are pentameric receptors composed of three sets of linked dimers with a "dangling" β2 subunit (Fig. 2 D). As it is unknown whether or how the linker dictates assembly, there are three possible ways in which such receptors can assemble with clockwise and counterclockwise orientations of the dimers (Fig. 2 D). Although this represents the simplest explanation, more complex assemblies including dangling α4 subunits or di-pentamers could also exist.

β-6-α and α4. Coinjection of β-6-α and α4 cRNA resulted in receptors of the 3α:2β stoichiometry. Based on visual inspection of the ACh CRR and an NS9283 response of 860%, the receptors appear identical to the ones obtained from α4 and β2 cRNA in a biased ratio, but also to those from the β-6-α dimer alone (ANOVA NS9283 response: F = 1.45, P = 0.25; Fig. 2, A–C; and Table 1). Given a known high propensity of monomeric subunits to integrate with linked subunits (Groot-Kormelink et al., 2004) and a 2:1 molar ratio of α4 to β-6-α in the cRNA mixture, it is reasonable to assume that the receptor pool in this case predominantly consists of "true" pentameric receptors (i.e., two sets of dimers with one monomeric α4 subunit).

β-6-α and $α4^{VFL}$. Robust ACh-evoked currents with amplitudes in the microampere range were observed upon coinjection of cRNA for β-6-α with monomeric $α4^{VFL}$; however, the resulting receptor pool did not appear related to any that were hitherto observed (Fig. 2, A–C; and Table 1). Judged from visual inspection of the ACh CRR, some resemblance was noted to receptors obtained with $α4^{VFL}$ and β2 cRNA in a biased ratio (Fig. 2 A). Yet, although both displayed biphasic ACh CRRs with similar $EC_{50}$ values, different first-component fractions led to altered curve progressions. Furthermore, an NS9283 response of 210% was observed for β-6-α and $α4^{VFL}$ in comparison to no positive efficacy with $α4^{VFL}$ and β2 (Fig. 2 B). Overall, these "intermittent" data point toward a mixed receptor pool containing subpopulations where some receptors are NS9283 sensitive and others are not. To rule out the presence of major receptor subpopulations with dangling subunits, we performed similar experiments with a 1:25 cRNA ratio of β-6-α and $α4^{VFL}$. In comparison with the 1:1 ratio, this did not significantly alter results for either ACh or NS9283 (Fig. 2, A and B). NS9283 gave rise to a 230% increase in $ACh_{control}$-evoked currents for the 1:25 ratio versus a 210% increase for the 1:1 ratio (*t* test NS9283 response: P = 0.49). This implies that receptors with dangling subunits do not constitute substantial subpopulations in the receptor pools.

Therefore, the receptor pool from β-6-α and $α4^{VFL}$ injection appears to consist primarily of pentamers from two linked dimers and one monomeric $α4^{VFL}$ subunit. Again, this is consistent with a known high propensity of monomeric subunits to integrate with linked subunits (Groot-Kormelink et al., 2004). Given that the data showed a mixed receptor pool with intermediate NS9283 response, these results could have only arisen from an ability of the linked dimers to orient themselves in both the clockwise and counterclockwise orientations. In total, there are four assembly possibilities in which the $α4^{VFL}$ subunit takes different positions between two dimers (Fig. 2 E). Of these four possibilities, one can likely be excluded, as it places all three α subunits consecutively (Fig. 2 E, right). Out of the remaining three, the scenario in which both dimers are oriented in the counterclockwise direction will lead to an α4–$α4^{VFL}$ interface that is insensitive to NS9283 (Fig. 2 E, left). In the remaining two scenarios, the VFL mutations are not facing the binding pocket of the α4–α4 interface, and the receptors formed are therefore still responsive to NS9283. Hence, the receptor pool arising from β-6-α and $α4^{VFL}$ injection contains at least two different receptor subpopulations, one sensitive and one insensitive to NS9283, and these can form only if the subunit assembly orientation is not directed by the construct.

### Increasing the number of linked subunits does not direct the orientation of linked subunits

Several studies with concatenated Cys-loop receptors have relied on linking more than two subunits (Baumann et al., 2002; Baur et al., 2006; Groot-Kormelink et al., 2006; Carbone et al., 2009; Kuryatov and Lindstrom, 2011; Shu et al., 2012; Jin et al., 2014; Mazzaferro et al., 2014). Having observed that the β-6-α construct does not direct the orientation of subunit assembly, we decided to investigate whether the addition of further linked subunits would affect this. We therefore used a previously published concatenated tetrameric construct, β2-6-α4-9-β2-6-α4, which was made by fusing two dimer β-6-α constructs to an $(AGS)_9$ linker (Carbone et al., 2009; Harpsøe et al., 2011). The three "extra" repeats used in comparison with the dimer

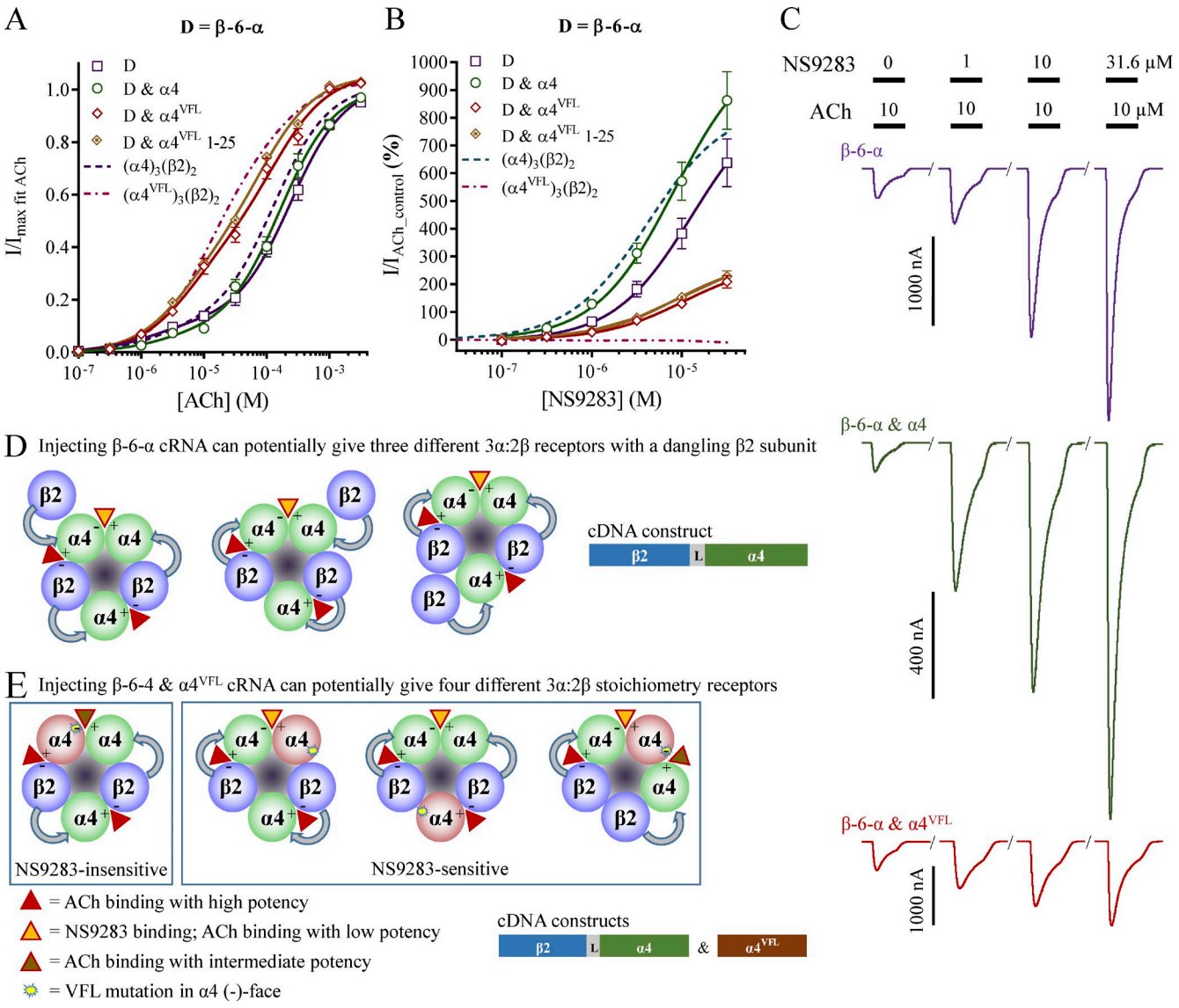


Figure 2. **ACh and NS9283 sensitivity and potential stoichiometry of receptors from the concatenated β-6-α construct.** *X. laevis* oocytes were subjected to two-electrode voltage-clamp electrophysiology as described in Materials and methods. **(A and B)** ACh (A) and NS9283 (B) CRRs were obtained from oocytes injected with the β-6-α dimer construct alone or coinjected with monomeric α4 or $\alpha4^{VFL}$ subunits in a 1:1 ratio. The linker sequence is shown in Table 3. Electrophysiological data were evaluated as described in Materials and methods; also see Fig. 1. Data from $n = 6–12$ experiments are depicted as means ± SEM as a function of the ACh or NS9283 concentration, and regression results are presented in Table 1. Data for wild-type receptors from monomeric subunits in Fig. 1 are indicated as dashed lines. **(C)** Representative traces illustrating NS9283 responses at oocytes injected with β-6-α, β-6-α and α4, or β-6-α and $\alpha4^{VFL}$. Bars above the traces indicate the 30-s application time and concentrations of applied compounds. **(D)** The simplest way in which a dimeric β-6-α construct could lead to functional 3α:2β stoichiometry receptors is three sets of linked dimers assembling with a dangling β2 subunit. This, again, could be envisioned to lead to three different assemblies because the two dimers in each receptor can be oriented in the clockwise, the counterclockwise, or both orientations when viewed from the synaptic cleft. Note that other, more complex assemblies cannot be excluded. **(E)** When coinjecting β-6-α and $\alpha4^{VFL}$, four different possible assemblies involving two dimer constructs and one monomeric subunit could arise. Of the four possibilities, one can likely be considered nonfunctional, given that all three α subunits are placed consecutively (right). If one or both dimers assemble in the clockwise orientation, the receptor will mimic wild-type 3α:2β receptors with respect to NS9283 sensitivity (middle). However, if both dimer constructs assemble in the counterclockwise orientation, the receptor will mimic wild-type 2α:3β receptors (left).

$(AGS)_6$ linker were included to compensate for the shorter C-terminal tail of α4 versus β2 to give similar linker lengths (Carbone et al., 2009). In the following results, the β2-6-α4-9-β2-6-α4 construct is termed β-6-α-9-β-6-α.

β-6-α-9-β-6-α. Relatively small $ACh_{max}$-evoked currents with amplitudes of ~50 nA were observed from oocytes injected with cRNA for β-6-α-9-β-6-α alone (Table 2). The receptor pool appeared to be a mixture containing

Table 2. **Maximal fitted response and potency of ACh and NS9283 from concatenated α4β2 nAChRs**

| Construct | Subunit | ACh | | | | | NS9283 | | | | Both |
|---|---|---|---|---|---|---|---|---|---|---|---|
| | | $E_{max}$ | $pEC_{50\_1}$ | $pEC_{50\_2}$ | Frac | *n* | $E_{31.6\ \mu M}$ | $E_{max}$ | $pEC_{50}$ | *n* | $ACh_{max}$ current |
| | | % | | | | | % | % | | | *nA* |
| α4 (10:1) | β2 | 102 ± 1 | 5.7 ± 0.3 | 3.9 ± 0.04 | 0.11 ± 0.03 | 14 | 760 ± 70 | 860 ± 60 | 5.3 ± 0.1 | 13 | 8,100 ± 900 (27) |
| $α4^{VFL}$ (10:1) | β2 | 104 ± 2 | 5.0 ± 0.1 | 3.9 ± 0.3 | 0.71 ± 0.12 | 9 | −9.9 ± 1.8 | No pos. pot. | N/A | 16 | 1,700 ± 300 (25) |
| Tetrameric | | | | | | | | | | | |
| β-6-α-9-β-6-α | | 109 ± 5 | 5.7 ± 0.2 | 3.8 ± 0.2 | 0.45 ± 0.07 | 6 | 170 ± 20 | 220 ± 30 | 5.0 ± 0.2 | 6 | 49 ± 9 (12) |
| β-6-α-9-β-6-α | α4 | 100 ± 1 | 5.9 ± 0.8 | 3.8 ± 0.04 | 0.035 ± 0.020 | 8 | 1,100 ± 100 | 1,300 ± 100 | 5.2 ± 0.1 | 6 | 1,500 ± 300 (14) |
| β-6-α-9-β-6-α | $α4^{VFL}$ | 109 ± 4 | 5.0 ± 0.2 | 3.6 ± 0.2 | 0.41 ± 0.09 | 9 | 130 ± 10 | 170 ± 20 | 5.0 ± 0.2 | 5 | 720 ± 130 (14) |
| β-6-α-9-β-6-α (1:5) | $α4^{VFL}$ | 102 ± 2 | 5.5 ± 0.3 | 4.2 ± 0.2 | 0.32 ± 0.13 | 13 | 100 ± 10 | 130 ± 20 | 5.1 ± 0.2 | 6 | 850 ± 170 (19) |
| β-6-α-9-β-6-α (1:25) | $α4^{VFL}$ | 106 ± 2 | 5.4 ± 0.1 | 4.0 ± 0.2 | 0.40 ± 0.12 | 9 | 130 ± 10 | 140 ± 10 | 5.4 ± 0.1 | 8 | 310 ± 40 (15) |
| Pentameric | | | | | | | | | | | |
| β-21a-α-β-α-α | | 101 ± 1 | 5.9 ± 0.3 | 3.7 ± 0.02 | 0.060 ± 0.011 | 12 | 930 ± 30 | 1,100 ± 40 | 5.1 ± 0.1 | 14 | 2,300 ± 400 (15) |
| β-21a-α-β-α-$α^{VFL}$ | | 105 ± 1 | 5.2 ± 0.1 | 4.0 ± 0.2 | 0.59 ± 0.07 | 14 | 41 ± 4 | 48 ± 5 | 5.3 ± 0.2 | 19 | 2,400 ± 400 (22) |
| β-21a-α-α-β-α | | 100 ± 2 | 6.1 ± 0.6 | 4.0 ± 0.05 | 0.060 ± 0.025 | 14 | 780 ± 90 | 910 ± 70 | 5.3 ± 0.1 | 9 | 5,300 ± 700 (23) |
| β-21a-α-$α^{VFL}$-β-α | | 102 ± 2 | 5.3 ± 0.2 | 4.3 ± 0.2 | 0.46 ± 0.18 | 19 | 55 ± 6 | 75 ± 9 | 5.0 ± 0.2 | 23 | 2,000 ± 200 (39) |
| β-21a-$α^{VFL}$-α-β-α | | 104 ± 1 | 5.2 ± 0.1 | 4.1 ± 0.1 | 0.44 ± 0.1 | 12 | 85 ± 10 | 102 ± 10 | 5.2 ± 0.1 | 12 | 600 ± 60 (12) |
| β-3a-α-β-α-α | | 102 ± 1 | 6.0 ± 0.3 | 4.0 ± 0.04 | 0.11 ± 0.02 | 9 | 640 ± 90 | 800 ± 90 | 5.1 ± 0.2 | 5 | 700 ± 120 (14) |
| β-3a-α-β-α-$α^{VFL}$ | | 104 ± 1 | 5.4 ± 0.1 | 4.3 ± 0.1 | 0.53 ± 0.08 | 14 | 11 ± 2 | 13 ± 1[a] | 5.8 ± 0.2 | 15 | 1,400 ± 400 (29) |
| β-3a-$α^{VFL}$-β-α-α | | 105 ± 1 | 5.6 ± 0.1 | 4.1 ± 0.1 | 0.39 ± 0.05 | 15 | 200 ± 20 | 240 ± 20 | 5.2 ± 0.1 | 9 | 440 ± 80 (24) |
| β-3a-$α^{VFL}$-α-β-α | | 105 ± 4 | 5.1 ± 0.3 | 3.6 ± 0.2 | 0.28 ± 0.10 | 9 | 270 ± 10 | 340 ± 20 | 5.1 ± 0.1 | 12 | 730 ± 120 (17) |

Data for ACh and NS9283 obtained from tetrameric or pentameric concatenated constructs are handled and presented as described in Table 1. Longer incubation times of 3–7 d were generally utilized to increase expression levels. Data for α4 and β2 or $α4^{VFL}$ and β2 are from Table 1 for reference purposes. No pos. pot., no positive potentiation.

[a]No NS9283 efficacy observed in ~50% of oocytes, resulting in poor fitting, as evidenced by the apparent increase in potency.

2α:3β and 3α:2β receptors with a fraction of 0.45 for the first ACh CRR component and an NS9283 response of 170% (Fig. 3, A and B; and Table 2). Hence, it is possible to form functional pentameric receptors from two linked tetramers, leaving three subunits dangling in at least two ways.

β-6-α-9-β-6-α and α4. As expected, coinjecting cRNA of β-6-α-9-β-6-α and monomeric α4 gave rise to receptors with ACh and NS9283 characteristics matching the wild-type 3α:2β stoichiometry receptors (Fig. 3, A and B; and Table 2). Mean $ACh_{max}$-evoked currents were in the 1–2-μA range, demonstrating that a tetrameric construct is an efficient way of generating standard binary 3α:2β receptors.

β-6-α-9-β-6-α and $α4^{VFL}$. Finally, when β-6-α-9-β-6-α and monomeric $α4^{VFL}$ cRNA were coinjected, the receptor pool appeared similar to that observed with the β-6-α and $α4^{VFL}$ combination, both with respect to their ACh CRR and NS9283 response (Fig. 3, A and B; and Tables 1 and 2). Although the difference in observed NS9283 response with 130% for β-6-α-9-β-6-α and $α4^{VFL}$ versus 210% for β-6-α and $α4^{VFL}$ was significant (*t* test NS9283 response: $P = 0.010$), both datasets reveal receptor pools mixed from NS9283-sensitive and NS9283-insensitive receptors. To evaluate whether subpopulations with dangling subunits constitute major contaminants, experiments were conducted using β-6-α-9-β-6-α and $α4^{VFL}$ cRNA ratios of 1:5 and 1:25. This represents a 20–100-fold molar surplus of the $α4^{VFL}$ subunit in the cRNA mixtures. Yet, the data for the three tested ratios were virtually identical to the NS9283 response, ranging from 100 to 130% (Fig. 3 B and Table 2). Thus, receptors formed from only linked tetramers with dangling subunits do not appear to be substantial subpopulations in the β-6-α-9-β-6-α and $α4^{VFL}$ receptor pools. The simplest explanation of the observed result is that linked subunits assemble readily in both clockwise and counterclockwise orientations, resulting in receptors with both NS9283-sensitive $α4^{VFL}$–α4 and NS9283-insensitive α4–$α4^{VFL}$ interfaces (Fig. 3 C).

Because linked tetramers assemble into functional receptors in both the clockwise and counterclockwise orientations, it appears unlikely that adding a fifth subunit would alter this flexibility. To verify this, we made two new pentameric constructs with a wild-type α4 or a mutant $α4^{VFL}$ subunit as the fifth and final subunit. These were termed β-21a-α-β-α-α and β-21a-α-β-α-$α^{VFL}$, and although not of identical sequence, the linkers largely resemble those in the previously published tetrameric β-6-α-9-β-6-α construct above (Table 3). The chosen nomenclature indicates the number of inserted amino acids (a) between the first two subunits.

β-21a-α-β-α-α. With only wild-type subunits in the pentameric construct, the ACh CRR and NS9283 response were, as expected, similar to those observed with α4 and β2 cRNA in a biased ratio (Fig. 3, D and E; and Table 2). The mean $ACh_{max}$-evoked currents were ~2 μA. This demonstrates that pentameric constructs can lead to expression levels equal to shorter linked constructs, but

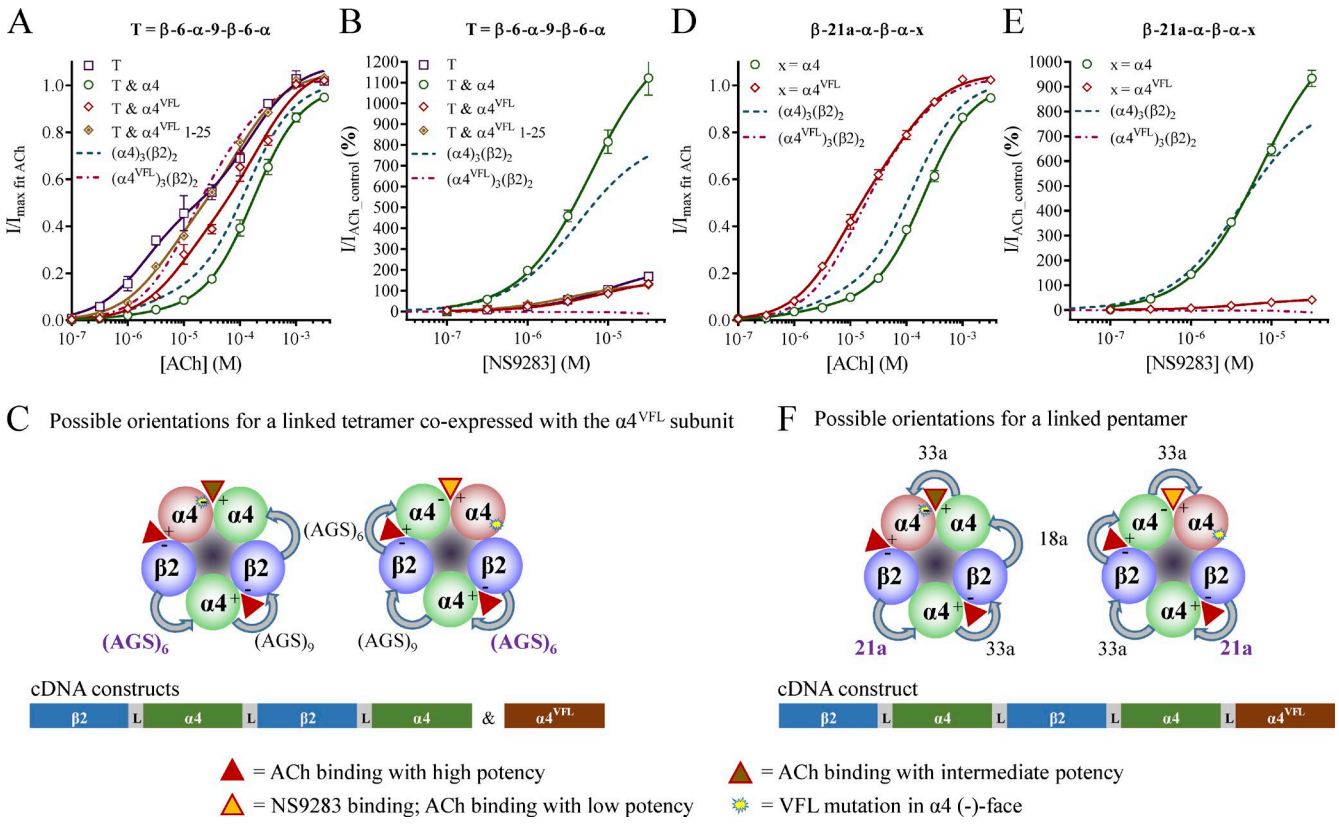


Figure 3. **ACh and NS9283 sensitivity and potential stoichiometry of receptors from concatenated tetrameric or pentameric constructs.** *X. laevis* oocytes were subjected to two-electrode voltage-clamp electrophysiology. Electrophysiological data were evaluated as described in Materials and methods; also see Fig. 1. **(A and B)** ACh (A) and NS9283 (B) CRRs were obtained from oocytes injected with the tetrameric β-6-α-9-β-6-α (T) construct alone or coinjected with monomeric α4 or $\alpha4^{VFL}$ subunits in a 1:1 ratio. Data from $n$ = 5–13 experiments are depicted as means ± SEM as a function of the ACh or NS9283 concentration, and regression results are presented in Table 2. Data for wild-type receptors from monomeric subunits in Fig. 1 are indicated as dashed lines. **(C)** Functional 3α:2β stoichiometry receptors arising from coinjections of β-6-α-9-β-6-α and $\alpha4^{VFL}$ could originate from assembly of the concatenated construct in either a clockwise or a counterclockwise orientation when viewed from the synaptic cleft. With respect to NS9283 sensitivity, receptors with the tetramer in the clockwise orientation will resemble wild-type 3α:2β receptors, whereas receptors with the tetramer in the counterclockwise orientation will resemble wild-type 2α:3β receptors. **(D and E)** ACh (D) and NS9283 (E) CRRs were obtained from oocytes injected with the indicated pentameric constructs, in which x indicates either the α4 or the $\alpha4^{VFL}$ subunit in the fifth construct position. Data from $n$ = 12–19 experiments are depicted as means ± SEM as a function of the ACh or NS9283 concentration, and regression results are presented in Table 2. **(F)** When injecting the pentameric construct including the $\alpha4^{VFL}$ subunit, clockwise and counterclockwise assemblies lead to different receptors, and NS9283 behaves differentially as described in C. Note that in the receptor illustrations, the first construct linkers are indicated with bold purple font, and specific linker sequences are shown in Table 3.

this requires increased incubation time after cRNA injection.

β-21a-α-β-α-$\alpha^{VFL}$. With the mutated $\alpha4^{VFL}$ as the final subunit in the pentameric complex, the data qualitatively resembled those from both the β-6-α and $\alpha4^{VFL}$ and β-6-α-9-β-6-α and $\alpha4^{VFL}$ combinations above. NS9283 modulation of expected potency was observed in all 19 tested oocytes for β-21a-α-β-α-$\alpha^{VFL}$, albeit a lower mean NS9283 response of 41% was observed for the pentameric construct compared with 100–130% for the tetrameric construct above. Nevertheless, the presence of NS9283-sensitive receptors suggests that linked pentamers assemble in both clockwise and counterclockwise orientations (Fig. 3 F).

### The position of the α4–α4 interface within a construct does not influence expression orientation

Because injection of a tetrameric construct alone can lead to functional receptors, it remains a possibility that the receptor pools in the β-6-α-9-β-6-α and $\alpha4^{VFL}$ and β-21a-α-β-α-$\alpha^{VFL}$ scenarios above contained small populations of receptors with dangling subunits. With the $\alpha4^{VFL}$ subunit either being a separate entity in the cRNA mixture or the final fifth subunit in the linked construct, it could be envisioned that minor receptor populations do not have this subunit included within their pentameric complex. Minor populations of receptors of only wild-type subunits might lead to an NS9283 response in the observed 41–130% range; this could therefore alter the conclusions. To examine this, we created three new,

Table 3. **Linker sequences utilized for creating concatenated α4β2 nAChR constructs**

| Linked set | Full name | C-term. | Linker sequence | Mature N term. | C tail | Linker | N term. (to L anchor) | Total |
|---|---|---|---|---|---|---|---|---|
| Dimeric constructs | | | | | | | | |
| β-6-α | β2-6-α4 | APSSK | $EG(AGS)_6R$ | AHAEE | 23 | 21 | 6 | 50 |
| β-9a-α | β2-9a-α4 | APSSK | $(AGS)_3$ | AHAEE | 23 | 9 | 6 | 38 |
| β-6a-α | β2-6a-α4 | APSSK | $(AGS)_2$ | AHAEE | 23 | 6 | 6 | 35 |
| β-3a-α | β2-3a-α4 | APSSK | AGS | AHAEE | 23 | 3 | 6 | 32 |
| β-0a-α | β2-0a-α4 | HSAPS | GS | AHAEE | 21 | 2 | 6 | 29 |
| β-(-3a)-α | β2-(-3a)-α4 | HSDHS | GS | AHAEE | 18 | 2 | 6 | 26 |
| Tetrameric and pentameric constructs | | | | | | | | |
| $\beta^1$-21a-$\alpha^2$- | $\beta2^1$-21a-$\alpha4^2$- | APSSK | $(AGS)_7$ | AHAEE | 23 | 21 | 6 | 50 |
| $\beta^1$-3a-$\alpha^2$- | $\beta2^1$-3a-$\alpha4^2$- | APSSK | AGS | AHAEE | 23 | 3 | 6 | 32 |
| -$\alpha^2$-$\beta^3$- | -$\alpha4^2$-33a-$\beta2^3$- | LAGMI | $(AGS)_5LGS(AGS)_5$ | TDTEE | 8 | 33 | 6 | 47 |
| -$\alpha^2$-$\alpha^3$- | -$\alpha4^2$-33a-$\alpha4^3$- | LAGMI | $(AGS)_5LGS(AGS)_5$ | AHAEE | 8 | 33 | 6 | 47 |
| -$\beta^3$-$\alpha^4$- | -$\beta2^3$-18a-$\alpha4^4$- | APSSK | $(AGS)_2AGT(AGS)_3$ | AHAEE | 23 | 18 | 6 | 47 |
| -$\alpha^3$-$\beta^4$- | -$\alpha4^3$-33a-$\beta2^4$- | LAGMI | $(AGS)_7ATG(AGS)_3$ | TDTEE | 8 | 33 | 6 | 47 |
| -$\alpha^4$-$\alpha^5$ | -$\alpha4^4$-33a-$\alpha4^5$ | LAGMI | $(AGS)_4ATG(AGS)_6$ | AHAEE | 8 | 33 | 6 | 47 |
| -$\beta^4$-$\alpha^5$ | -$\beta2^4$-20a-$\alpha4^5$ | APSSK | $TG(AGS)_6$ | AHAEE | 23 | 20 | 6 | 49 |

The five most proximal C-terminal (C-term.) amino acids and the five first amino acids from the predicted mature N terminus (N term.) are presented for α4 and β2 subunits along with the specific linker sequences introduced during concatenation. C-terminal tail lengths were obtained from NCBI (SwissProt accession nos. P43681 for α4 and P17787 for β2), whereas N-terminal lengths were derived from the definition of an α-helical hydrophobic leucine anchor as described in the Results. For tetrameric and pentameric constructs, numbers indicate the construct position of each subunit (e.g., $\alpha^2$: α4 subunit in the second construct position).

additional pentameric constructs in which the α4–α4 interface was placed in the construct center: β-21a-α-α-β-α, β-21a-α-$\alpha^{VFL}$-β-α, and β-21a-$\alpha^{VFL}$-α-β-α (Table 3). Interestingly, similar constructs were previously found to express very poorly (Carbone et al., 2009); however, no plausible reason for this finding was provided.

β-21a-α-α-β-α. When the pentameric construct containing only wild-type subunits was expressed in oocytes, the ACh and NS9283 CRRs revealed a receptor pool of archetypical 3α:2β stoichiometry receptors (Fig. 4, A–C; and Table 2). The NS9283 response of 780% for β-21a-α-α-β-α was not significantly different from the 760% observed with receptors obtained from the expression of monomeric subunits using a biased ratio (*t* test NS9283 response: P = 0.86). The mean maximal current amplitude of 5.3 µA for β-21a-α-α-β-α matched and even surpassed that of previously tested pentameric constructs, contrasting with the observations of Carbone et al. (2009). This indicates that the specific position of the α4–α4 motif within a pentameric construct has no particular impact on surface expression levels.

β-21a-α-$\alpha^{VFL}$-β-α. The ACh CRR showed greater resemblance to receptors from monomeric $\alpha4^{VFL}$ and β2 when the pentameric construct contained an $\alpha4^{VFL}$ subunit in the third construct position (Fig. 4 A). Nevertheless, with an NS9283 response of 55%, the receptor pool clearly contained both sensitive and insensitive receptors (Fig. 4, B and C; and Table 2). Given the construct position of the $\alpha4^{VFL}$ subunit, sensitive receptors must have their linkers in a clockwise orientation in this scenario (Fig. 4 D, top).

β-21a-$\alpha^{VFL}$-α-β-α. Data for the pentameric construct with the $\alpha4^{VFL}$ subunit in the second position were virtually identical to those observed for $\alpha4^{VFL}$ in the third position, as described in the previous paragraph. The ACh CRR resembled that of monomeric $\alpha4^{VFL}$ and β2 (Fig. 4 A), and an NS9283 response of 85% revealed a mixed receptor pool (Fig. 4, B and C; and Table 2). Because of the construct position of the $\alpha4^{VFL}$ subunit, NS9283-sensitive receptors must have their linkers in the counterclockwise orientation in this scenario (Fig. 4 D, bottom).

It is relatively easy to imagine how a pentameric construct could "loop out" the first or the last construct subunit and assemble into functional receptors from two or more pentamers with dangling subunits. However, it is difficult to envision how pentameric constructs with an $\alpha4^{VFL}$ subunit placed in the center could assemble into functional receptors without the inclusion of the $\alpha4^{VFL}$ subunit. All three tested pentameric constructs showed similar NS9283 responses in the range of 41–85%; hence, the collective data demonstrate that linked pentamers readily assemble in both orientations.

### Is it possible for linkers to direct the assembly orientation of Cys-loop receptors?

Given the aforementioned data, it is essential to theoretically assess whether it is at all possible to direct the assembly orientation using subunit concatenation. The linker connects the C-terminal tail extruding from transmembrane helix four (TM4) of the first subunit to the mature N terminus of the second subunit. There appears to be no inherent proficiency of the first subunit to significantly influence the linker direction. Despite having a long C-terminal tail in comparison with

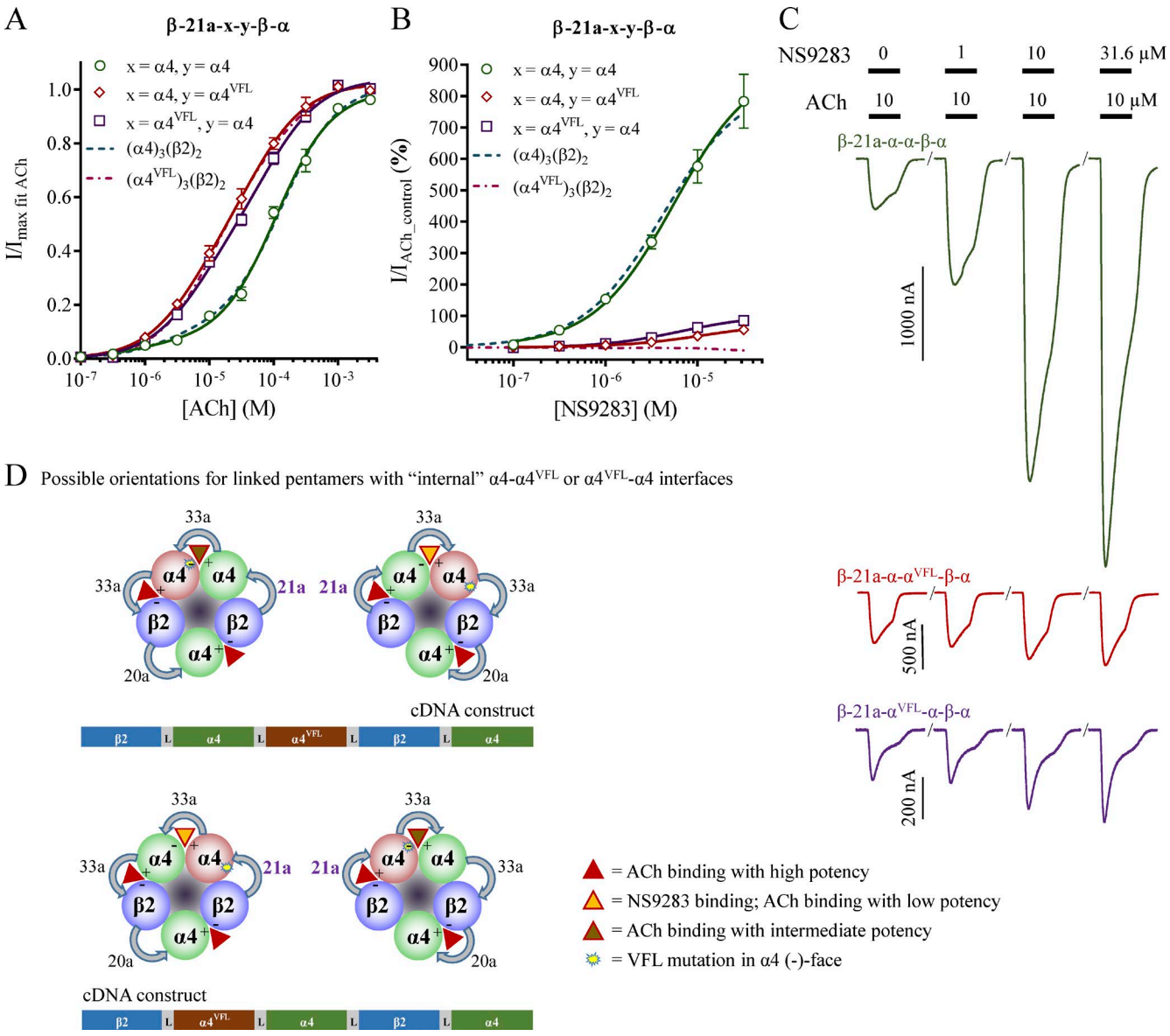


Figure 4. **ACh and NS9283 sensitivity and potential stoichiometry of receptors from concatenated pentameric constructs with the α4–α4 site in the second to third construct positions.** *X. laevis* oocytes were subjected to two-electrode voltage-clamp electrophysiology. Electrophysiological data were evaluated as described in Materials and methods; also see Fig. 1. **(A and B)** ACh (A) and NS9283 (B) CRRs were obtained from oocytes injected with the indicated pentameric constructs, where x and y denote an α4 or an $α4^{VFL}$ subunit in the second and third construct positions. Data from $n$ = 9–23 experiments are depicted as means ± SEM as a function of the ACh or NS9283 concentration, and regression results are presented in Table 2. Data for wild-type receptors from monomeric subunits in Fig. 1 are indicated as dashed lines. **(C)** Representative traces illustrating NS9283 responses at oocytes injected with β-21a-α-α-β-α, β-21a-α-$α^{VFL}$-β-α, or β-21a-$α^{VFL}$-α-β-α. Bars above the traces indicate the 30-s application time and concentrations of applied compounds. **(D)** For the β-21a-α-$α^{VFL}$-β-α receptor ($α4^{VFL}$ subunit in the third construct position), NS9283-sensitive receptors originate from assembly of the linkers in a clockwise orientation (top right). However, for the β-21a-$α^{VFL}$-α-β-α receptor ($α4^{VFL}$ subunit in the second construct position), NS9283-sensitive receptors are assembled with the linkers in a counterclockwise orientation (bottom left). Note that in the receptor illustrations, the first construct linkers are indicated with bold purple font, and specific linker sequences are shown in Table 3.

other nAChR subunits, a linked β2 tail easily orients itself in both directions. The flexibility of this part of the protein is supported by a lack of electron densities associated with the last 20 amino acids in the recently published α4β2 nAChR x-ray structure (Morales-Perez et al., 2016). Hence, for linking purposes, the C-terminal tail could simply be considered as part of the linker, and any potential control of the assembly orientation would rely on the structural features of the second subunit.

The extracellular domain of all Cys-loop subunits has an α-helical segment a few amino acids downstream of the mature N terminus, which points in the clock-

wise direction when viewed from the extracellular side (Fig. 5 A). The exact length and predicted number of α-helical turns vary between subunits, but the orientation of the helix is well defined. Based on the α4β2 x-ray structure, this helix is firmly attached to the remainder of the subunit through a series of conserved hydrophobic segments. These are termed LLxxLF in α4 and LVxxLL in β2, and both anchor into hydrophobic pockets on the subunits (Fig. 5 B). The hydrophobic patches ensure that the upstream N terminus remains pointed toward the complementary face of the subunit. Based on the 5KXI structure, the direct distance from the last amino acid in transmembrane segment four of β2 ($Leu^{479}$) to the N-terminal tip of mature α4 ($Ala^{34}$) in counterclockwise and clockwise directions is 61 and 81 Å, respectively. In reality, the distance on the surface of the protein is longer, so to give a more realistic estimate, we used molecular modeling to estimate the lowest number of AGS repeats required to connect β2 ($Leu^{479}$) to α4 ($Ala^{34}$) without causing significant distortions after energy minimization. This modeling approach used the linker as a flexible ruler and estimated that 8 and 10 AGS repeats were sufficient to connect the two terminals in the counterclockwise and clockwise directions (Fig. 5 C). This translates into a proposed difference in distance between the two orientations corresponding to approximately six amino acids or 20 Å. We therefore hypothesized that a clockwise orientation of linked subunits requires a longer minimal linker sequence than the counterclockwise one. This suggests that it is possible to obtain a uniform population of receptors in the counterclockwise orientation once the linker is sufficiently short.

### Strategy and design of new concatenated dimer constructs

When designing concatenated constructs with defined linker lengths, it is necessary to devise a strategy for calculating existing N- and C-terminal amino acids, as many of these end up as de facto parts of the linker. Calculating the length of the C-terminal tail is a straightforward process, as TM4 is well defined. For the N terminus, however, there is no obvious fix point from which to count "protruding" amino acids. Based on an alignment of all Cys-loop $GABA_AR$ and nAChR subunits, we define an N-terminal fix point as the first hydrophobic anchor in the α-helical segment mentioned in the previous paragraph; the conserved leucine corresponds to the first L in $L^{32}$VEHLL for β2 and $L^{40}$LKKLF for α4 (Fig. 5 B). The number of amino acids preceding this leucine in the proposed mature nAChR peptides varies from subunit to subunit. It can even vary for a given subunit depending on the predicted signal peptide cleavage. Out of 16 mammalian nAChR subunits, 8 (α1, α3, α7, β1, β2, ε, γ, and δ) have six amino acids preceding the leucine anchor; therefore, it appears reasonable to set six amino acids as a consensus for this receptor class. With this definition, mature β2 starts with $T^{26}$DTEE and α4 with $A^{34}$HAEE, which closely matches what was used by Zhou et al. (2003).

By strict definition, the linker in the original β-6-α construct is not only six AGS repeats but $EG(AGS)_6R$, as extra amino acids were added for restriction site purposes. Using our calculation method, the total linker length in β-6-α is 50 amino acids, and the linkers used for the new pentameric β-21a-α-β-α-α construct above had a length of 47–50 amino acids (Fig. 5 D and Table 3). To avoid the introduction of charged amino acids when designing new concatenated dimer constructs, we used primarily AGS repeats. Five new constructs were designed with total linker lengths of 38, 35, 32, 29, and 26 amino acids corresponding to the introduction of 9, 6, 3, 0, and −3 amino acids (Fig. 5 D and Table 3). These linker lengths span the predicted distances from the modeling. For clarity, a new nomenclature of β-xa-α was used, where x denotes the number of added amino acids (a).

### Shortened β-xa-α linkers can lead to a fixed counterclockwise orientation of linked subunits

β-9a-α. Injection of only β-9a-α cRNA into oocytes led to robust ACh-evoked currents, albeit with a fivefold loss of mean peak current amplitudes from 1,000 to 220 nA when compared with the β-6-α construct above (Table 1). Although the ACh CRR was best approximated by a biphasic equation, the fraction of the first component increased from 0.11 to 0.28, and the NS9283 response decreased from 640 to 100% (Fig. 6, A–C; and Table 1). Collectively, these changes suggest that the receptor pool contained a higher proportion of receptors in the 2α:3β stoichiometry when the dimer linker was shortened. Data from coinjections with α4 or $α4^{VFL}$ cRNA were very similar to the corresponding β-6-α data above, with an NS9283 response at 200% for β-9a-α and $α4^{VFL}$ versus 210% for β-6-α and $α4^{VFL}$. Hence, the β-9a-α linker was still long enough to allow assembly in both orientations (Fig. 6 D).

β-6a-α. The most noticeable impact observed from shortening the linker by one AGS repeat was fewer oocytes responding robustly to ACh applications when only cRNA for β-6a-α was injected (Table 1). Although the ACh CRR for β-6a-α and $α4^{VFL}$ did display closer visual resemblance to that of $α4^{VFL}$ and β2 from monomeric subunits, the NS9283 response was still substantial at 140% (Fig. 6, A–C; and Table 1), demonstrating assembly in both orientations (Fig. 6 D).

β-3a-α. In contrast, further shortening by one AGS repeat to create the β-3a-α construct yielded significantly different data. When cRNA for β-3a-α was injected alone, only one out of four oocytes responded to ACh

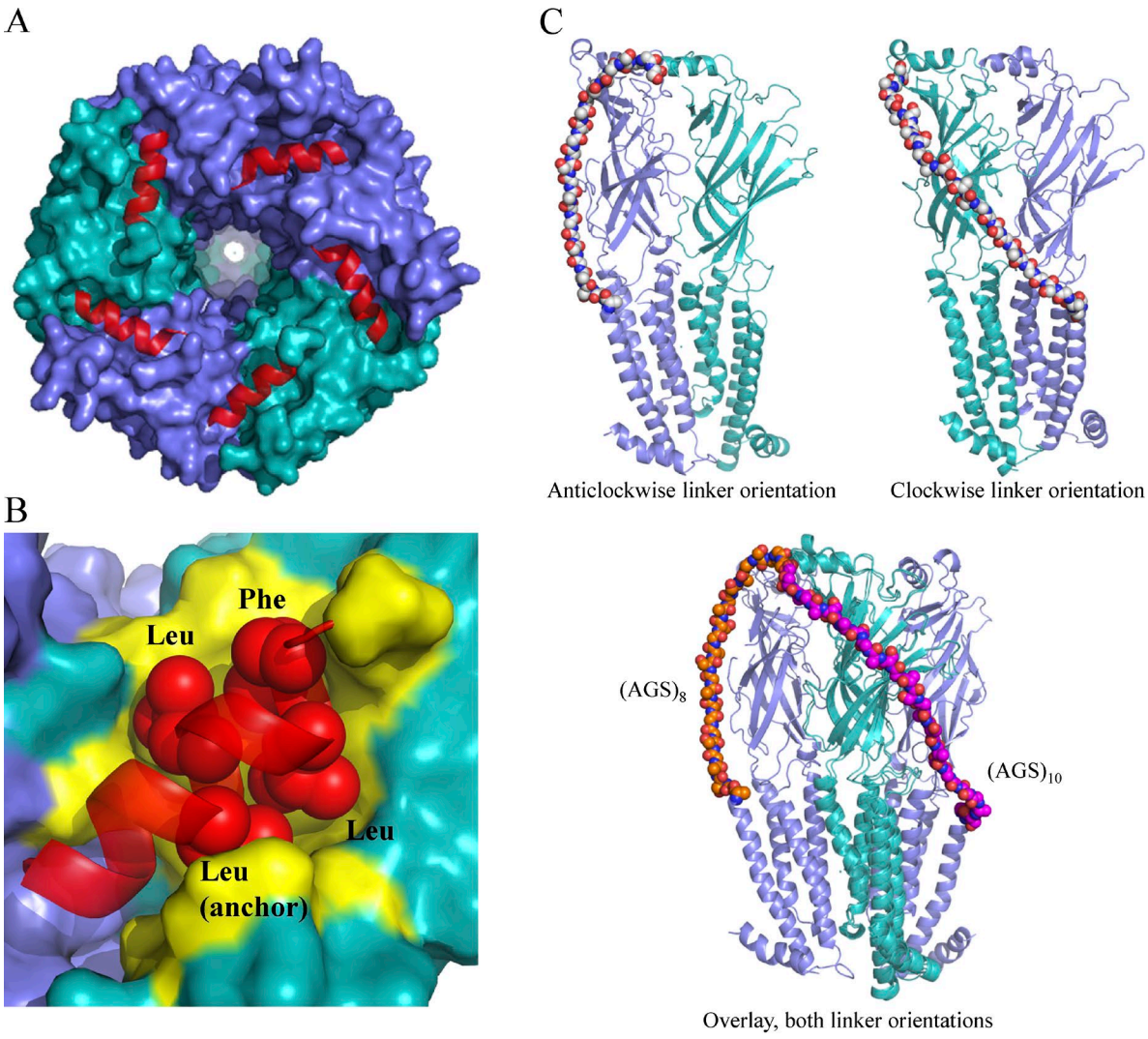


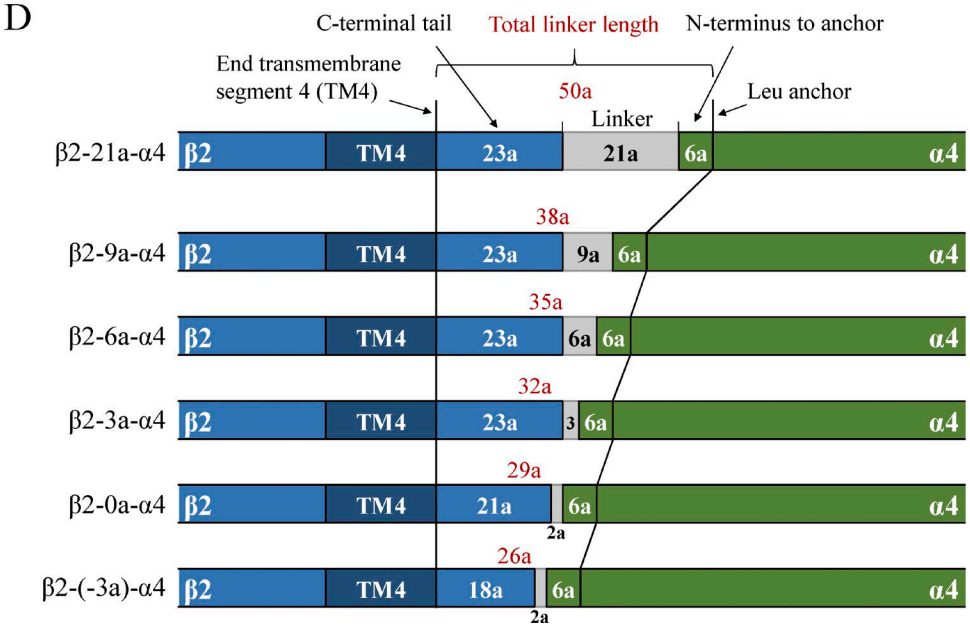

applications with low current amplitudes. Although coinjections with $\alpha4^{VFL}$ yielded receptors with robust ACh-evoked currents, these displayed low responsiveness to NS9283 with a response of 22% (Fig. 6, A–C; and Table 1). This indicates that the receptor pool contained linked dimers primarily, but not exclusively, in the counterclockwise orientation (Fig. 6 D). Importantly, this preference was accomplished without a detrimental loss of ACh-evoked current amplitudes or changes in the NS9283 response of the 3α:2β receptors obtained by coinjection of β-3a-α and α4 (Table 1).

β-0a-α. Additional shortening of the linker to create the β-0a-α construct resulted in a substantial loss of maximal ACh-evoked current amplitudes for all three tested cRNA mixtures. Therefore, additional incubation of the oocytes for 2–3 d was necessary to obtain current amplitudes >100 nA for an $ACh_{max}$ application. Nevertheless, the ACh and NS9283 responsiveness of oocytes coinjected with β-0a-α and α4 appeared identical to that of wild-type 3α:2β stoichiometry receptors, indicating that the linked dimer retains normal functionality. Remarkably, coinjection of β-0a-α and $\alpha4^{VFL}$ yielded receptors that appeared identical to those from monomeric $\alpha4^{VFL}$ and β2 subunits in a biased ratio (Fig. 6, A–C; and Table 1). No hint of NS9283 enhancement was noted in individual oocytes ($n$ = 15), which demonstrated an exclusive counterclockwise dimer orientation (Fig. 6 D).

β-(-3a)-α. As expected based on the data for the β-0a-α construct, removing an additional three amino acids from the linker to create the β-(−3a)-α construct aggravated issues with current amplitudes. Although ACh-evoked currents were observed (Table 1), they rarely approached the amplitudes necessary to perform full CRRs for ACh and NS9283 (set at >100 nA for an initial $ACh_{max}$ application).

Thus, when the total linker length in a dimer construct is shortened to 32 amino acids or less (Table 3), the resulting receptor pool predominantly contains receptors assembled from dimers in the counterclockwise orientation. This proves the hypothesis that a counterclockwise orientation represents the shortest distance for a linked construct. However, the data also indicate that obtainment of exclusive counterclockwise expression comes at a cost of low current amplitudes. For practical purposes, it may be advantageous to accept the risk of a small polluting receptor population.

### Pentameric constructs with one short linker express primarily in the counterclockwise orientation

Given that a shortened dimer construct expresses predominantly in the counterclockwise orientation, the same should theoretically also be applicable for pentameric constructs. Two points are worth noting in this context. First, when creating concatenated constructs of more than two subunits, it is logical to assume that if the first linker directs the orientation, subsequent linked subunits can only extend in the same direction. The used linkers are simply not long enough to bridge across several subunits, as would be required for altering direction. Second, if a linker is optimized to ensure only one assembly direction, it is likely to be tightly packed to the bridging subunits. This implies that a linker could pack tightly across the C loop of an agonist-binding interface, which intuitively should be avoided, as it may influence normal binding and function of the receptor. Therefore, when designing new constructs, we chose to use a total length of 32 amino acids for the first linker and keep the length of consecutive linkers at 47 amino acids (Table 3). Although a 32–amino acid linker did not lead to exclusive counterclockwise expression with the β-3a-α construct, it was deemed the best compromise, as pentameric constructs can be expected to give overall lower current amplitudes. The two new constructs were β-3a-α-β-α-α and β-3a-α-β-α-$\alpha^{VFL}$.

β-3a-α-β-α-α. When cRNA for β-3a-α-β-α-α was injected into oocytes, the resulting receptors appeared identical to those of wild-type 3α:2β stoichiometry from monomeric α4 and β2 in a biased ratio. With an NS9283 response of 640%, no significant difference ($t$ test NS9283 response: P = 0.36) was noted, compared with the 760% observed at 3α:2β stoichiometry receptors (Fig. 7, A and B; and Table 2).

β-3a-α-β-α-$\alpha^{VFL}$. In contrast, receptors in oocytes injected with the β-3a-α-β-α-$\alpha^{VFL}$ construct resembled those from monomeric $\alpha4^{VFL}$ and β2. The mean NS9283 response was 11%; however, it is noteworthy that no effect was observed in ∼25% of the oocytes. This indicates that the receptor pool for β-3a-α-β-α-$\alpha^{VFL}$ is dominated by receptors expressed in the counterclockwise orientation.

Figure 5. **3-D structure of the human α4β2 nAChR (from Protein Data Bank accession no.** 5KXI**; Morales-Perez et al., 2016) showing direction of N-terminal α-helix and modeled linkers.** The α4 subunit is colored green, and β2 is blue. **(A)** Top view of the $(\alpha4)_2(\beta2)_3$ receptor with the N-terminal helixes shown in red. **(B)** Top view of the α4β2 dimer with the N-terminal LLxxLF motif shown as red spheres. The surface of the protein constituting hydrophobic residues on the top of the α4 and β2 subunits is colored yellow. The LLxxLF motif interacts with the hydrophobic surface to form a hydrophobic patch. **(C)** α4β2 dimer with modeled long clockwise and short counterclockwise linkers. The shortest possible number of AGS repeats required to connect the first residue after TM4 of the β2 subunit ($Leu^{479}$) to the mature N terminus of α4 ($Ala^{34}$) is shown and had lengths of 10 and 8 repeats, respectively. **(D)** Illustration of total linker length calculations for new concatenated β-xa-α dimer constructs. Note that only parts of the cDNA sequences close to the linkers are shown.

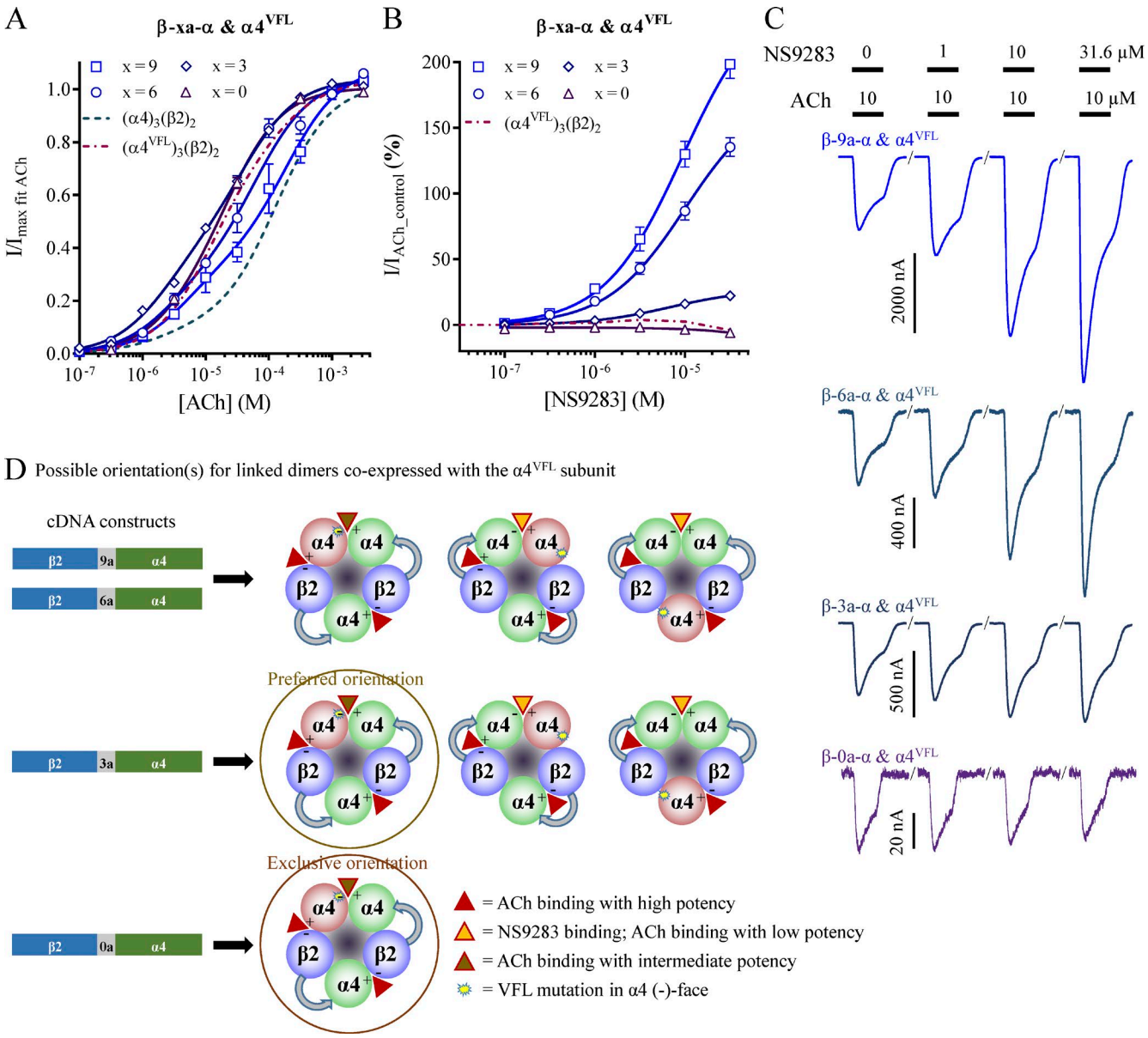


Figure 6. **ACh and NS9283 sensitivity and potential stoichiometry of receptors from concatenated β-xa-α dimer constructs.** *X. laevis* oocytes were subjected to two-electrode voltage-clamp electrophysiology. Electrophysiological data were evaluated as described in Materials and methods; also see Fig. 1. **(A and B)** ACh (A) and NS9283 (B) CRRs were obtained from oocytes coinjected with β-xa-α and the monomeric $\alpha4^{VFL}$ subunit in a 1:1 ratio. X represents the number of amino acids in the linker, and specific linker sequences are shown in Table 3. Data from $n$ = 5–24 experiments are depicted as means ± SEM as a function of the ACh or NS9283 concentration, and regression results are presented in Table 1. Data for the receptor obtained from monomeric $\alpha4^{VFL}$ and β2 subunits in Fig. 1 are indicated with dashed lines. **(C)** Representative traces illustrating NS9283 responses at oocytes injected with β-9a-α and $\alpha4^{VFL}$, β-6a-α and $\alpha4^{VFL}$, β-3a-α and $\alpha4^{VFL}$, or β-0a-α and $\alpha4^{VFL}$. Bars above the traces indicate the 30-s application time and concentrations of applied compounds. **(D)** Based on the lack of NS9283 efficacy observed in B, receptors originating from coinjection of β-0a-α with the monomeric $\alpha4^{VFL}$ subunit have the concatenated construct assembled exclusively in the counterclockwise orientation when viewed from the synaptic cleft.

### Substituting an α4 with an $\alpha4^{VFL}$ subunit in each position in an $(\alpha4)_3(\beta2)_2$ receptor

With a methodology for expressing pentamers in a preferred orientation, it becomes possible to evaluate the effects of introducing an $\alpha4^{VFL}$ subunit in each of the three possible positions in a 3α:2β stoichiometry receptor. Data for $\alpha4^{VFL}$ in the complementary side position of the α4–$\alpha4^{VFL}$ interface are addressed by the β-3a-α-β-α-$\alpha^{VFL}$ construct in the previous paragraph. To investigate the other two positions, two new pentameric constructs were made: β-3a-$\alpha^{VFL}$-β-α-α (wild-type α4–α4 interface) and β-3a-$\alpha^{VFL}$-α-β-α ($\alpha4^{VFL}$–α4 interface).

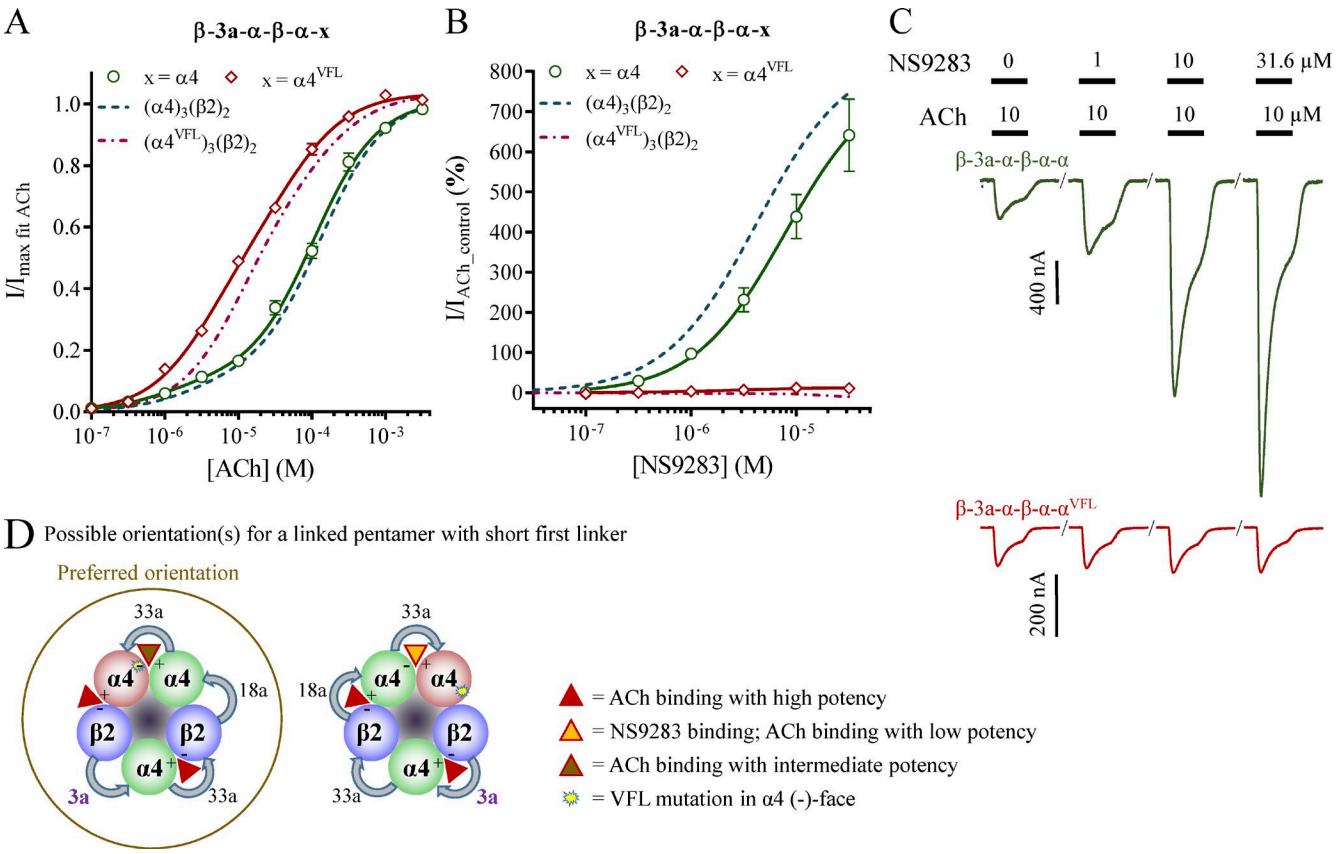


Figure 7. **ACh and NS9283 sensitivity and potential stoichiometry of receptors from concatenated pentameric constructs with short first linkers.** *X. laevis* oocytes were subjected to two-electrode voltage-clamp electrophysiology. Electrophysiological data were evaluated as described in Materials and methods; also see Fig. 1. **(A and B)** ACh (A) and NS9283 (B) CRRs were obtained from oocytes injected with the indicated pentameric constructs in which x denotes an α4 or an $\alpha4^{VFL}$ subunit in the fifth construct position. Data from $n$ = 5–15 experiments are depicted as means ± SEM as a function of the ACh or NS9283 concentration, and regression results are presented in Table 2. Data for wild-type receptors from monomeric subunits in Fig. 1 are indicated as dashed lines. **(C)** Representative traces illustrating NS9283 responses at oocytes injected with β-3a-α-β-α-α (top) or β-3a-α-β-α-$\alpha^{VFL}$ (bottom). Bars above the traces indicate the 30-s application time and concentrations of applied compounds. **(D)** Based on the NS9283 responses observed with x = $\alpha4^{VFL}$ in B, the receptor pool consists mainly of pentamers with the linkers assembled in the counterclockwise orientation when viewed from the synaptic cleft. Note that in the receptor illustrations, the first construct linkers are indicated with bold purple font, and specific linker sequences are shown in Table 3.

β-3a-$\alpha^{VFL}$-β-α-α. When the $\alpha4^{VFL}$ subunit is placed between two β2 subunits, the three mutations are located in the complementary side of a β2–$\alpha4^{VFL}$ interface, and because of the construct symmetry, this is not dependent on expression orientation. As β2–α4 interfaces are not believed to bind ACh, it would be expected that the mutations have no effect on an ACh CRR. If this was the case, the ACh CRR should look similar to that of wild-type 3α:2β stoichiometry receptors; however, as first noted by Lucero et al. (2016), this is in fact not the case. Instead, the ACh CRR visually appeared more similar to that of $\alpha4^{VFL}$ and β2, albeit the fitted parameters for $EC_{50}$ values and fractions were not identical (Fig. 8 A and Table 2). How mutations in a nonbinding interface can exert such an effect is presently unclear. Nevertheless, the β-3a-$\alpha^{VFL}$-β-α-α receptors remained sensitive to NS9283 binding in the α4–α4 interface (Fig. 8 B and Table 2). The observed response of 250% could seem low compared with wild-type 3α:2β stoichiometry receptors, but this is to be expected because a fixed $ACh_{control}$ concentration of 10 μM was used in all experiments (~$EC_{40}$ for β-3a-$\alpha^{VFL}$-β-α-α receptors vs. ~$EC_{15}$ for α4 and β2).

β-3a-$\alpha^{VFL}$-α-β-α. Finally, with the construct in which the preferred counterclockwise orientation leads to $\alpha4^{VFL}$–α4 interfaces, the ACh CRR visually most resembled that of wild-type 3α:2β stoichiometry receptors (Fig. 8 A). That said, the fitted parameters were not identical, and in particular, the fraction of the first component of the curve was almost threefold higher (Table 2). Presumably, this was because of the presence of a small population of receptors expressed in the clockwise orientation, which showed higher sensitivity to low ACh concentrations. With an observed NS9283 response of 270%, the receptors responded less than

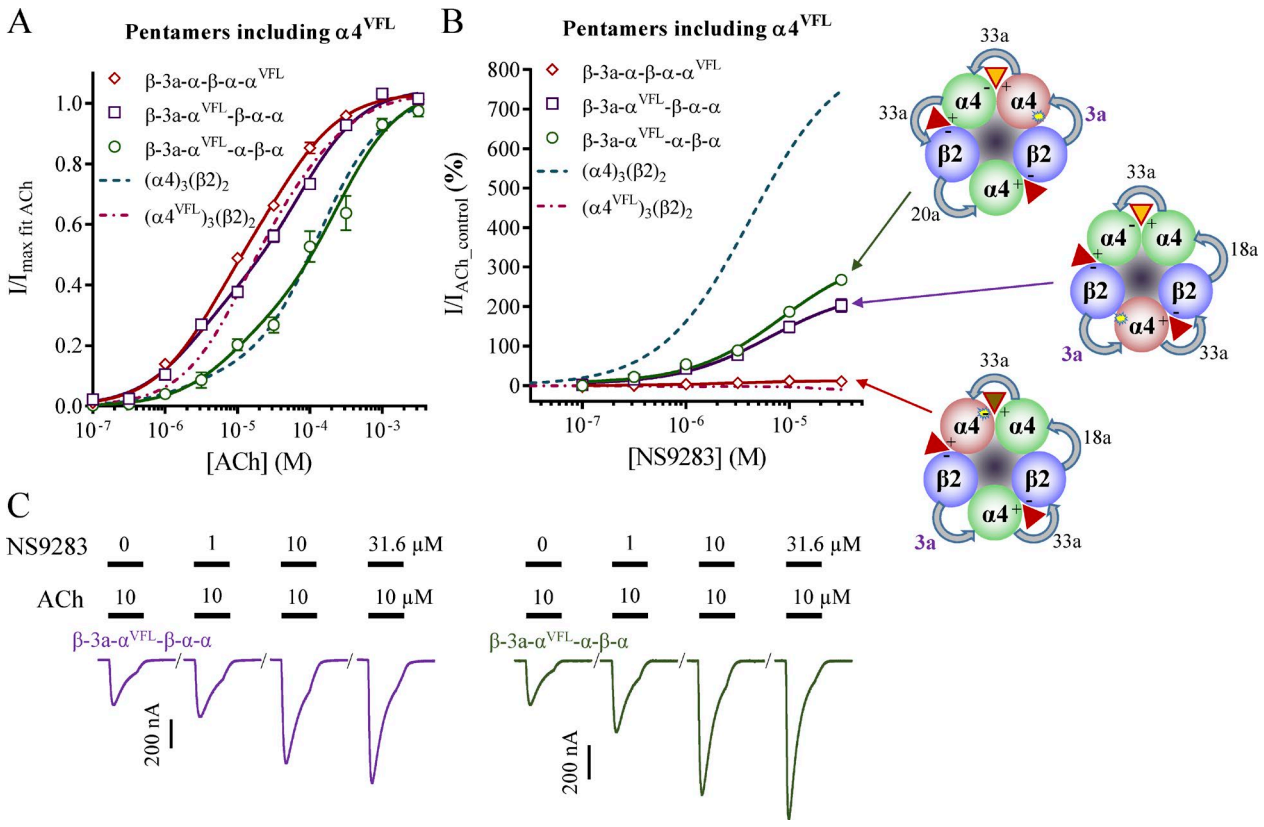


Figure 8. **ACh and NS9283 sensitivity of receptors from α4$^{VFL}$ subunit containing concatenated pentameric constructs with short first linkers.** *X. laevis* oocytes were subjected to two-electrode voltage-clamp electrophysiology. Electrophysiological data were evaluated as described in Materials and methods; also see Fig. 1. **(A and B)** ACh (A) and NS9283 (B) CRRs were obtained from oocytes injected with the indicated pentameric constructs. Data from $n$ = 9–15 experiments are depicted as means ± SEM as a function of the ACh or NS9283 concentration, and regression results are presented in Table 2. Data for the β-3a-α-β-α-α$^{VFL}$ construct are from Fig. 7, and data for wild-type receptors from monomeric subunits in Fig. 1 are indicated as dashed lines. The preferred expression orientation of each pentamer is indicated for the NS9283 data. **(C)** Representative traces illustrating NS9283 responses at oocytes injected with β-3a-α$^{VFL}$-β-α-α or β-3a-α$^{VFL}$-α-β-α. Bars above the traces indicate the 30-s application time and concentrations of applied compounds.

wild-type 3α:2β stoichiometry receptors (Fig. 8 B and Table 2). There could be two reasons for this: (1) the presence of a population of receptors that did not respond to NS9283, or (2) the α4$^{VFL}$–α4 interface might not have responded to NS9283 fully like a wild-type α4–α4 interface does. The higher first component fraction of the ACh CRR and the fact that NS9283 displayed normal potency in the α4$^{VFL}$–α4 interface suggest that the first reason is more likely.

## DISCUSSION

For heteromeric Cys-loop receptors, the method of subunit concatenation holds great promise. Theoretically, this technique allows for detailed experimental control at the single-subunit level that would not otherwise be possible. In reality, when working with α4β2 nAChR–concatenated constructs based on published designs, we observed that the resulting receptor pools were not always uniform. Although the technique worked superbly for wild-type binary receptors, this was not the case for ternary receptors (including binary receptors with mutations in one of the subunits, which technically make them ternary receptors). In this study, we therefore investigated to what degree a concatenation strategy can be used to direct subunit assembly and what is required for this to work reliably.

The β-6-α construct first published by Zhou et al. (2003) exemplifies a case in which ternary receptors can convolute the data. Coexpression with a monomeric α4$^{VFL}$ subunit clearly resulted in a mixed receptor pool, as evidenced from the response to NS9283. The most plausible explanation is that receptor subpopulations arose from dimer assembly in clockwise, counterclockwise, or both directions. Assuming no linker direction bias, this could lead to a receptor pool containing four different ternary receptors. The exact percentage of these different receptor types is not easily established; however, the data support the notion of at least two abundant receptor subpopulations. Although it might be speculated that increasing the number of linked subunits in the cDNA construct would alleviate

the problem, this was not the case. NS9283 data for the previously published (Carbone et al., 2009; Harpsøe et al., 2011) tetrameric β-6-α-9-β-6-α construct coexpressed with a monomeric $\alpha4^{VFL}$ subunit or a similarly designed fully pentameric β-21a-α-β-α-$\alpha^{VFL}$ construct still revealed mixed receptor pools. Furthermore, new pentameric constructs with the $\alpha4^{VFL}$ subunit positioned in the construct center (β-21a-α-$\alpha^{VFL}$-β-α and β-21a-$\alpha^{VFL}$-α-β-α) also led to mixed receptor pools. Hence, it can be concluded that typically used concatenated α4β2 constructs do not ensure expression of pure ternary receptor pools, as the linked subunits can assemble readily in both orientations.

When evaluating models of Cys-loop receptors, it is clear that the C-terminal tail is a flexible entity with no specific features that are likely to significantly direct subunit assembly orientation. This is in good agreement with data for the β-6-α construct, and for linking purposes, it is therefore sensible to consider the C-terminal tail merely as part of the linker sequence. Although it is easy to determine the length of a C-terminal tail based on TM4, it is less straightforward to predict the length of a corresponding N-terminal "protrusion." We defined the first amino acid of mature nAChR subunits and total linker lengths based on a hydrophobic anchor in the α-helical segment located at the top of all Cys-loop receptor subunits. In this context, perhaps the most important feature of this α-helical segment was the fact that it was pointing in a clockwise direction when viewed from the synaptic cleft. This brought the N terminus toward the subunit complementary face and caused a difference in length between a linker bridging the TM4 of one subunit to the N terminus of the next subunit in the clockwise versus the counterclockwise direction. Our calculations suggested that the clockwise linker should be approximately six amino acids longer than the counterclockwise one. Hence, we hypothesized that a uniform receptor pool with concatenated constructs expressing only in the counterclockwise orientation is attainable when the linkers are short.

To evaluate whether a shorter linker would direct subunit assembly, we decreased the total calculated linker length of dimer constructs progressively from 38 down to 26 amino acids, 3 amino acids at a time. Based on this, it appeared that a linker of 35 amino acids was too long (substantial NS9283 response), whereas a linker of 26 amino acids was too short (peak current amplitudes that were too low). The "sweet spot" appeared to be a linker length of ∼32 amino acids. The β-3a-α dimer showed a low NS9283 response when coexpressed with the $\alpha4^{VFL}$ subunit, but showed wild-type 3α:2β stoichiometry behavior when coexpressed with the α4 subunit. This demonstrates that the receptor pool has dimers primarily oriented in the counterclockwise direction. Although a small subpopulation with dimers in the clockwise orientation was present, this appeared sufficiently negligible for most practical purposes. Hence, our hypothesis that an optimized short linker can direct dimer subunit assembly was proven experimentally.

Having discovered that 32 amino acids represent a good compromise for a dimeric construct linker length, we next evaluated whether this would also be applicable for pentameric constructs. Three constructs were made in which a single $\alpha4^{VFL}$ subunit replaced a wild-type α4 subunit in each of the three possible locations in the 3α:2β stoichiometry receptor. Importantly, a low NS9283 response (11%) was observed at the receptor containing an α4–$\alpha4^{VFL}$ interface versus a substantial response (270%) at the receptor with an $\alpha4^{VFL}$–α4 interface. This demonstrates that pentameric constructs, like their dimeric counterparts, express in a preferred counterclockwise orientation when the first construct linker is 32 amino acids. Again, it is important to note that although this linker length might represent a good compromise, it did not ensure a 100% uniform receptor population.

When considering the experimental data for the shortened dimeric constructs, it appears that the actual difference between a linker traversing the clockwise versus the counterclockwise orientation was less than what had been predicted from the 3-D x-ray structures. Exclusive counterclockwise orientation was only observed with finely optimized short linkers, and the margin between exclusivity and loss of function appeared narrow in the order of a few amino acids. Hence, the models likely overestimated the real distance difference, most likely because of the flexibility of TM4 and potential unwinding of the helices, which had not been observed in the experimentally determined structure.

The consequences of these findings are substantial. The β-6-α construct contains a total linker length of 50 amino acids (using our calculation method), and similar linkers have been used to design various concatenated constructs in laboratories across the world. This raises fundamental questions as to the validity of published data whenever resulting receptors are of a ternary nature. There are many examples in which this was the case: (a) concatenated dimeric or pentameric constructs were used to show that the α5 subunit can occupy two positions in the $(\alpha4\beta2)_2\alpha5$ receptor, either as a nonbinding subunit or as a replacement of one β2 subunit (Jin et al., 2014); (b) by introducing point mutations and expressing a dimer construct with monomeric subunits, Jain et al. (2016) concluded that both α5 and β3 can participate in what was termed "unorthodox ACh-binding sites"; (c) pentameric constructs were used to show that the role or equality of subunits differ, depending on their specific positions within the α4β2 receptor complex (Mazzaferro et al., 2014); and (d) by introducing point mutations in the β2 subunit, Lucero et al. (2016) concluded that the two canonical α4–β2 ACh agonist sites make significantly different contributions

to receptor activation for α4β2 receptors in the 2α:3β (but not the 3α:2β) stoichiometry. However, all of these studies correspond to ternary receptor scenarios, and in the absence of strong evidence regarding linker orientation, the respective conclusions may be erroneous.

Given the extensive use of the concatenation technology, it is puzzling that the complexity of this technique is not widely recognized. One explanation for this lies in the data resolution with which many constructs have been studied. Fundamentally, ACh CRRs, biphasic ones in particular, rarely yield data of sufficient resolution to determine whether a receptor pool is truly uniform. Another explanation relates to the prior use of ambiguous data to draw conclusions. Zhou et al. (2003) attempted to determine the assembly orientation of their constructs by coexpression with the β4 subunit and evaluating for a cytisine response. They concluded that linked β-6-α dimers express in a clockwise orientation; however, this relied on speculation regarding expected cytisine responses from receptors with mixed α4–β2 and α4–β4 agonist interfaces. Therefore, to ensure sufficient resolution and unambiguous data, we relied on the site-selective agonism of NS9283. At the highest tested concentrations of NS9283 (31.6 µM), an $EC_{15}$ ACh-evoked current is increased by ∼700%. This allows for robust detection of even a low percentage of responding receptors in pools of primarily nonresponding receptors.

Prior observations with $GABA_A$Rs support that the findings observed in this study are likely to be universal to all Cys-loop receptors. Baumann et al. (2001) elegantly applied concatenated receptors to answer fundamental questions regarding the stoichiometry of an α1β2γ2 receptor. Although their linker lengths were shorter than typical nAChR linkers (37–41 vs. 50 amino acids using our calculation method), occurrence of GABA-evoked currents with some construct combinations (e.g., αβ/γ) can only be explained by dimers expressing in both orientations. Hence, for $GABA_A$Rs, similar considerations will have to be considered when evaluating data.

### Conclusion

In the present study, we demonstrate that typically used linker lengths in concatenated nAChR constructs do not ensure uniform receptor expression of ternary receptors. This is because the linked subunits can orient themselves readily in both the clockwise and the counterclockwise directions. For ternary or more complex scenarios, this leads to receptor pools containing mixed stoichiometries. By shortening construct linkers, it is possible to use concatenation to ensure expression of receptor pools with a preference toward subunits in a counterclockwise orientation. However, substantial optimization is required to obtain exclusive expression for a given set of subunits. This is because linker length changes of only a few angstroms can make a substantial difference. Consequently, it is of the utmost importance to carefully assess the used concatenated constructs when evaluating the validity of historical data or when designing new experiments.

## ACKNOWLEDGMENTS

We wish to thank Troels E. Sørensen for insightful discussions.

This work was conducted as part of an Australian Research Council Linkage project in collaboration with Bionomics Limited. This work was supported by Bionomics Limited, the Australian Research Council (grant LP140100781), and the Australian National Health and Medical Research Council (grant APP1069417).

The authors declare no competing financial interests.

Author contributions: P.K. Ahring designed the research. V.W.Y. Liao, P.K. Ahring, and T. Balle performed the research. P.K. Ahring analyzed the data and drafted the manuscript. All authors approved the final version of the manuscript.

Richard W. Aldrich served as editor.

Submitted: 11 July 2017
Revised: 15 November 2017
Accepted: 22 December 2017

## REFERENCES

Ahring, P.K., L.H. Bang, M.L. Jensen, D. Strøbæk, L.Y. Hartiadi, M. Chebib, and N. Absalom. 2016. A pharmacological assessment of agonists and modulators at α4β2γ2 and α4β2δ GABAA receptors: The challenge in comparing apples with oranges. *Pharmacol. Res.* 111:563–576. https://doi.org/10.1016/j.phrs.2016.05.014

Baumann, S.W., R. Baur, and E. Sigel. 2001. Subunit arrangement of gamma-aminobutyric acid type A receptors. *J. Biol. Chem.* 276:36275–36280. https://doi.org/10.1074/jbc.M105240200

Baumann, S.W., R. Baur, and E. Sigel. 2002. Forced subunit assembly in alpha1beta2gamma2 GABAA receptors. Insight into the absolute arrangement. *J. Biol. Chem.* 277:46020–46025. https://doi.org/10.1074/jbc.M207663200

Baur, R., F. Minier, and E. Sigel. 2006. A GABA(A) receptor of defined subunit composition and positioning: concatenation of five subunits. *FEBS Lett.* 580:1616–1620. https://doi.org/10.1016/j.febslet.2006.02.002

Berman, H.M., T. Battistuz, T.N. Bhat, W.F. Bluhm, P.E. Bourne, K. Burkhardt, Z. Feng, G.L. Gilliland, L. Iype, S. Jain, et al. 2002. The Protein Data Bank. *Acta Crystallogr. D Biol. Crystallogr.* 58:899–907. https://doi.org/10.1107/S0907444902003451

Carbone, A.L., M. Moroni, P.J. Groot-Kormelink, and I. Bermudez. 2009. Pentameric concatenated (alpha4)(2)(beta2)(3) and (alpha4)(3)(beta2)(2) nicotinic acetylcholine receptors: subunit arrangement determines functional expression. *Br. J. Pharmacol.* 156:970–981. https://doi.org/10.1111/j.1476-5381.2008.00104.x

Groot-Kormelink, P.J., S.D. Broadbent, J.P. Boorman, and L.G. Sivilotti. 2004. Incomplete incorporation of tandem subunits in recombinant neuronal nicotinic receptors. *J. Gen. Physiol.* 123:697–708. https://doi.org/10.1085/jgp.200409042

Groot-Kormelink, P.J., S. Broadbent, M. Beato, and L.G. Sivilotti. 2006. Constraining the expression of nicotinic acetylcholine receptors by using pentameric constructs. *Mol. Pharmacol.* 69:558–563. https://doi.org/10.1124/mol.105.019356

Harpsøe, K., P.K. Ahring, J.K. Christensen, M.L. Jensen, D. Peters, and T. Balle. 2011. Unraveling the high- and low-sensitivity agonist responses of nicotinic acetylcholine receptors. *J. Neurosci.* 31:10759–10766. https://doi.org/10.1523/JNEUROSCI.1509-11.2011

Indurthi, D.C., T.M. Lewis, P.K. Ahring, T. Balle, M. Chebib, and N.L. Absalom. 2016. Ligand Binding at the 4-4 Agonist-Binding Site of the 42 nAChR Triggers Receptor Activation through a Pre-Activated Conformational State. *PLoS One.* 11:e0161154. https://doi.org/10.1371/journal.pone.0161154

Jain, A., A. Kuryatov, J. Wang, T.M. Kamenecka, and J. Lindstrom. 2016. Unorthodox Acetylcholine Binding Sites Formed by α5 and β3 Accessory Subunits in α4β2* Nicotinic Acetylcholine Receptors. *J. Biol. Chem.* 291:23452–23463. https://doi.org/10.1074/jbc.M116.749150

Jin, X., and J.H. Steinbach. 2011. A portable site: a binding element for 17β-estradiol can be placed on any subunit of a nicotinic α4β2 receptor. *J. Neurosci.* 31:5045–5054. https://doi.org/10.1523/JNEUROSCI.4802-10.2011

Jin, X., I. Bermudez, and J.H. Steinbach. 2014. The nicotinic α5 subunit can replace either an acetylcholine-binding or nonbinding subunit in the α4β2* neuronal nicotinic receptor. *Mol. Pharmacol.* 85:11–17. https://doi.org/10.1124/mol.113.089979

Kaur, K.H., R. Baur, and E. Sigel. 2009. Unanticipated structural and functional properties of delta-subunit-containing GABAA receptors. *J. Biol. Chem.* 284:7889–7896. https://doi.org/10.1074/jbc.M806484200

Kuryatov, A., and J. Lindstrom. 2011. Expression of functional human α6β2β3* acetylcholine receptors in Xenopus laevis oocytes achieved through subunit chimeras and concatamers. *Mol. Pharmacol.* 79:126–140. https://doi.org/10.1124/mol.110.066159

Lucero, L.M., M.M. Weltzin, J.B. Eaton, J.F. Cooper, J.M. Lindstrom, R.J. Lukas, and P. Whiteaker. 2016. Differential alpha4(+)/(-)beta2 Agonist-binding Site Contributions to alpha4beta2 Nicotinic Acetylcholine Receptor Function within and between Isoforms. *J. Biol. Chem.* 291:2444–2459. https://doi.org/10.1074/jbc.M115.684373

Mazzaferro, S., N. Benallegue, A. Carbone, F. Gasparri, R. Vijayan, P.C. Biggin, M. Moroni, and I. Bermudez. 2011. Additional acetylcholine (ACh) binding site at alpha4/alpha4 interface of (alpha4beta2)2alpha4 nicotinic receptor influences agonist sensitivity. *J. Biol. Chem.* 286:31043–31054. https://doi.org/10.1074/jbc.M111.262014

Mazzaferro, S., F. Gasparri, K. New, C. Alcaino, M. Faundez, P. Iturriaga Vasquez, R. Vijayan, P.C. Biggin, and I. Bermudez. 2014. Non-equivalent ligand selectivity of agonist sites in (α4β2)2α4 nicotinic acetylcholine receptors: a key determinant of agonist efficacy. *J. Biol. Chem.* 289:21795–21806. https://doi.org/10.1074/jbc.M114.555136

Mirza, N.R., J.S. Larsen, C. Mathiasen, T.A. Jacobsen, G. Munro, H.K. Erichsen, A.N. Nielsen, K.B. Troelsen, E.O. Nielsen, and P.K. Ahring. 2008. NS11394 [3′-[5-(1-hydroxy-1-methyl-ethyl)-benzoimidazol-1-yl]-biphenyl-2-carbonitrile], a unique subtype-selective GABAA receptor positive allosteric modulator: in vitro actions, pharmacokinetic properties and in vivo anxiolytic efficacy. *J. Pharmacol. Exp. Ther.* 327:954–968. https://doi.org/10.1124/jpet.108.138859

Morales-Perez, C.L., C.M. Noviello, and R.E. Hibbs. 2016. X-ray structure of the human α4β2 nicotinic receptor. *Nature.* 538:411–415. https://doi.org/10.1038/nature19785

Olsen, J.A., J.S. Kastrup, D. Peters, M. Gajhede, T. Balle, and P.K. Ahring. 2013. Two distinct allosteric binding sites at α4β2 nicotinic acetylcholine receptors revealed by NS206 and NS9283 give unique insights to binding activity-associated linkage at Cys-loop receptors. *J. Biol. Chem.* 288:35997–36006. https://doi.org/10.1074/jbc.M113.498618

Olsen, J.A., P.K. Ahring, J.S. Kastrup, M. Gajhede, and T. Balle. 2014. Structural and functional studies of the modulator NS9283 reveal agonist-like mechanism of action at α4β2 nicotinic acetylcholine receptors. *J. Biol. Chem.* 289:24911–24921. https://doi.org/10.1074/jbc.M114.568097

Shu, H.J., J. Bracamontes, A. Taylor, K. Wu, M.M. Eaton, G. Akk, B. Manion, A.S. Evers, K. Krishnan, D.F. Covey, et al. 2012. Characteristics of concatemeric GABA(A) receptors containing α4/δ subunits expressed in Xenopus oocytes. *Br. J. Pharmacol.* 165:2228–2243. https://doi.org/10.1111/j.1476-5381.2011.01690.x

Timmermann, D.B., K. Sandager-Nielsen, T. Dyhring, M. Smith, A.M. Jacobsen, E.O. Nielsen, M. Grunnet, J.K. Christensen, D. Peters, K. Kohlhaas, et al. 2012. Augmentation of cognitive function by NS9283, a stoichiometry-dependent positive allosteric modulator of α2- and α4-containing nicotinic acetylcholine receptors. *Br. J. Pharmacol.* 167:164–182. https://doi.org/10.1111/j.1476-5381.2012.01989.x

Zhou, Y., M.E. Nelson, A. Kuryatov, C. Choi, J. Cooper, and J. Lindstrom. 2003. Human alpha4beta2 acetylcholine receptors formed from linked subunits. *J. Neurosci.* 23:9004–9015 (PubMed).

Zwart, R., and H.P. Vijverberg. 1998. Four pharmacologically distinct subtypes of alpha4beta2 nicotinic acetylcholine receptor expressed in Xenopus laevis oocytes. *Mol. Pharmacol.* 54:1124–1131. https://doi.org/10.1124/mol.54.6.1124